BRAIN
REVIEW ARTICLE

Imaging chronic active lesions in multiple sclerosis: a consensus statement

Francesca Bagnato,[1,2] Pascal Sati,[3] Christopher C. Hemond,[4] Colm Elliott,[5] Susan A. Gauthier,[6] Daniel M. Harrison,[7,8] Caterina Mainero,[9] Jiwon Oh,[10] David Pitt,[11] Russell T. Shinohara,[12,13] Seth A. Smith,[14] Bruce Trapp,[15] Christina J. Azevedo,[16] Peter A. Calabresi,[17] Roland G. Henry,[18] Cornelia Laule,[19,20,21,22] Daniel Ontaneda,[23] William D. Rooney,[24] Nancy L. Sicotte,[25] Daniel S. Reich[26] and Martina Absinta[17,27], on behalf of the NAIMS Cooperative

Chronic active lesions (CAL) are an important manifestation of chronic inflammation in multiple sclerosis and have implications for non-relapsing biological progression. In recent years, the discovery of innovative MRI and PET-derived biomarkers has made it possible to detect CAL, and to some extent quantify them, in the brain of persons with multiple sclerosis, *in vivo*.

Paramagnetic rim lesions on susceptibility-sensitive MRI sequences, MRI-defined slowly expanding lesions on T_1-weighted and T_2-weighted scans, and 18-kDa translocator protein-positive lesions on PET are promising candidate biomarkers of CAL. While partially overlapping, these biomarkers do not have equivalent sensitivity and specificity to histopathological CAL. Standardization in the use of available imaging measures for CAL identification, quantification and monitoring is lacking.

To fast-forward clinical translation of CAL, the North American Imaging in Multiple Sclerosis Cooperative developed a consensus statement, which provides guidance for the radiological definition and measurement of CAL. The proposed manuscript presents this consensus statement, summarizes the multistep process leading to it, and identifies the remaining major gaps in knowledge.

1 Neuroimaging Unit, Neuroimmunology Division, Department of Neurology, Vanderbilt University Medical Center, Nashville, TN 37212, USA
2 Department of Neurology, Nashville VA Medical Center, Tennessee Valley Healthcare System, Nashville, TN 37212, USA
3 Neuroimaging Program, Department of Neurology, Cedars-Sinai Medical Center, Los Angeles, CA 90048, USA
4 Department of Neurology, University of Massachusetts Chan Medical School, Worcester, MA 01655, USA
5 NeuroRx Research, Montréal, QC H2X 3P9, Canada
6 Department of Neurology, Weill Cornell Medicine, New York, NY 10021, USA
7 Department of Neurology, University of Maryland School of Medicine, Baltimore, MD 21201, USA
8 Department of Neurology, Baltimore VA Medical Center, VA Maryland Healthcare System, Baltimore, MD 21201, USA
9 Athinoula A. Martinos Center for Biomedical Imaging, Department of Radiology, Massachusetts General Hospital, Harvard Medical School, Boston, MA 02115, USA
10 Division of Neurology, St. Michael's Hospital, University of Toronto, Toronto, ON M5S, Canada
11 Department of Neurology, Yale School of Medicine, New Haven, CT 06510, USA
12 Penn Statistics in Imaging and Visualization Endeavor, Department of Biostatistics, Epidemiology, and Informatics, Perelman School of Medicine, University of Pennsylvania, Philadelphia, PA 19104, USA
13 Center for Biomedical Image Computing and Analytics, Department of Radiology, Perelman School of Medicine, University of Pennsylvania, Philadelphia, PA 19104, USA

Received March 21, 2023. Revised November 21, 2023. Accepted December 08, 2023. Advance access publication January 16, 2024

14 Department of Radiology and Radiological Sciences, Vanderbilt University Institute of Imaging Science, Vanderbilt University Medical Center, Nashville, TN 37235, USA
15 Department on Neurosciences, Lerner Research Institute, Cleveland Clinic, Cleveland, OH 44195, USA
16 Department of Neurology, Keck School of Medicine of the University of Southern California, Los Angeles, CA 90007, USA
17 Departments of Neurology and Neuroscience, Johns Hopkins University School of Medicine, Baltimore, MD 21205, USA
18 Weill Institute for Neurosciences, Department of Neurology, University of California, San Francisco, CA 94158, USA
19 Department of Radiology, University of British Columbia, Vancouver, BC V6T 1Z4, Canada
20 Department of Pathology & Laboratory Medicine, University of British Columbia, Vancouver, BC V6T 1Z4, Canada
21 Department of Physics and Astronomy, University of British Columbia, Vancouver, BC V6T 1Z4, Canada
22 International Collaboration on Repair Discoveries (ICORD), University of British Columbia, Vancouver, BC V6T 1Z4, Canada
23 Mellen Center for Multiple Sclerosis, Cleveland Clinic, Cleveland, OH 44195, USA
24 Advanced Imaging Research Center, Oregon Health and Science University, Portland, OR 97239, USA
25 Department of Neurology, Cedars-Sinai Medical Center, Los Angeles, CA 90048, USA
26 Translational Neuroradiology Section, National Institute of Neurological Disorders and Stroke, National Institutes of Health, Bethesda, MD 20892, USA
27 Translational Neuropathology Unit, Division of Neuroscience, Institute of Experimental Neurology, Vita-Salute San Raffaele University and IRCCS San Raffaele Scientific Institute, Milan, 20132, Italy

Correspondence to: Francesca Bagnato, MD, PhD
Neuroimaging Unit, Neuroimmunology Division, Department of Neurology
Vanderbilt University Medical Center, 2201 Children's Way, Suite 1222, Nashville, TN, 37212, USA
E-mail: francesca.r.bagnato@vanderbilt.edu

Keywords: chronic active lesions; iron; microglia; multiple sclerosis; paramagnetic rim lesions; MRI-defined slowly evolving lesions

Introduction

Acute inflammatory brain and spinal cord white matter lesions featuring blood–brain barrier breakdown[1] are a cardinal feature of multiple sclerosis (MS).[2] Acute white matter lesions are visible on T_1-weighted MRI obtained upon the administration of gadolinium-based contrast agent (GBCA).[3] Acute inflammatory activity is associated with relapses[4] and predicts short-term disease outcome.[5]

Once acute white matter inflammation resolves, they may evolve into chronic active lesions (CAL)[6] or chronic inactive lesions, or they may remyelinate.[7] CAL (sometimes referred to as mixed active/inactive or smouldering) can be detected not only in the brain white matter but also in cortical regions[8] and in the spinal cord.[9,10] CAL are an important manifestation of chronic inflammation in multiple sclerosis,[11] representing focal areas of compartmentalized inflammation trapped within the CNS behind a relatively intact blood–brain barrier.[12]

Post-mortem studies indicate that CAL predominate in patients with multiple sclerosis and progressive disease,[13,14] particularly in those with a shorter time to disability accumulation.[15] Furthermore, the proportion of CAL was seen to be a strong predictor of both disease severity and lesion burden.[15] Thus, neuropathological evidence indicates that chronic inflammation has implications for non-relapsing biological progression and functional outcome of patients with multiple sclerosis.[13–15]

The increasingly recognized role of chronic inflammation in multiple sclerosis has challenged the view of multiple sclerosis phenotypes[16,17] and led to a new, biologically driven framework for reclassifying this disease.[17] Identifying chronic inflammation *in vivo*, using non-invasive imaging methods, will likely underlie future efforts to personalize treatments and stratify patients for more efficient clinical trials of treatments targeting progressive biology.

Despite these advances, CAL assessment is not routinely implemented in day-to-day clinical practice and has only recently been included in clinical trials. Lack of standardization in CAL identification, quantification and monitoring is the main constraint to clinical translation. To fast-forward clinical translation of CAL, the North American Imaging in Multiple Sclerosis Cooperative (NAIMS)[18] developed this consensus statement, which provides guidance for the radiological definition and measurement of CAL and identifies remaining major gaps in knowledge. This consensus statement was conceptualized by several subject-matter experts via a multistep process. A summary is provided in the Supplementary material.

Materials and methods

On 23 February 2022, experts on the use of MRI and PET in patients with multiple sclerosis, along with multiple sclerosis clinicians and scientists, convened at a workshop[19] in West Palm Beach, FL, USA. The meeting was organized by a subcommittee of NAIMS and was attended by representatives from nearly all NAIMS sites.

Prior to the meeting, the organizing committee identified five major aspects of imaging CAL *in vivo* as important topics for discussion: (i) paramagnetic rim lesions (PRLs) and their role as a surrogate measure of CAL; (ii) slowly expanding lesions (SELs) and their accuracy in reflecting CAL and PRLs; (iii) PET and its ability to identify CAL and PRLs; (iv) the overall relationship between PRLs, SELs or

18-kDa translocator protein (TSPO) lesions and disability; and (v) the role of these biomarkers in disease prognostication.

Experts were invited to discuss current knowledge on several facets of these topics. All members of the organizing committee reviewed and discussed each presentation in advance and drafted a preliminary consensus statement on each topic.

On the day of the meeting, each invited presenter discussed the state of knowledge on the selected themes. Thereafter, the organizing committee proposed its preliminary consensus statements and identified knowledge gaps. These were debated by all presenters and workshop participants, and a final collective agreement was established. Care was taken to discuss each opinion difference extensively and in detail, to ensure that the final statement was reflective of any disagreement resolution.

After the meeting, the organizing committee, referred to as the 'panel' hereafter, reviewed each presentation along with the related discussions, the final consensus reached on the day of the workshop, and the identified knowledge gaps. These were drafted into this manuscript by the first author and all presenters. The first draft was then critically reviewed and appropriately modified by: (i) each member of the workshop organizing committee and the NAIMS steering committee at the time of the workshop; (ii) each presenter; and (iii) workshop participants and experts who substantially contributed to the discussion during the meeting.

Microglia/astrocyte phenotypes in chronic white matter lesions

Formation of acute white matter lesions is associated with the transient influx of peripheral immune cells, which penetrate the CNS through an altered blood–brain barrier and produce demyelination, reactive gliosis, neuroaxonal compromise and secondarily, myelin debris removal.[11] Active lesions feature the presence of CD68+ phagocytes, including blood-derived macrophages and activated microglia, throughout the entire lesion core.[11] On the contrary, CAL have a hypocellular core with scarce macrophages and microglia.[11] A salient feature of CAL is iron-laden microglia at the lesion border, a factor that determines their unique visibility on magnetic susceptibility-sensitive MRI. On histopathology, the microglia rim may not always surround the lesion core in its entirety.[6,11] Some CAL show signs of 'ongoing' demyelination (defined by the presence of myelin debris in phagocytosing cells). In the literature, this feature has defined 'smouldering lesions'. According to some authors, actively demyelinating lesions can be further classified into early demyelinating lesions, featured by the presence of major and small molecular weight myelin proteins inside macrophages, and late demyelinating lesions, whose macrophages only contain major myelin proteins.[11] Small molecular weight myelin proteins include the cyclic nucleotide diphosphoesterase (CNPase), myelin oligodendrocyte glycoprotein (MOG), and myelin-associated glycoprotein (MAG). Major myelin proteins are myelin basic protein (MBP) and proteolipid protein (PLP).[11]

Glia have a predominant, yet poorly defined role in the pathophysiology of chronic white matter lesions. Single cell and single nucleus RNA-sequencing (RNA-seq) studies identified multiple glial phenotypes in chronic multiple sclerosis lesions.[20–23] A single nucleus RNA-seq study[23] focused especially on CAL identified two multiple sclerosis-associated microglia populations with a TREM2-APOE gene expression signature, partially overlapping with those described in animal models of Alzheimer's disease. One of these populations appeared to be prevalently involved in myelin phagocytosis and clearance, whereas the other showed high expression of major histocompatibility complex (MHC), and inflammation, as well as iron-related genes, consistent with the observed iron accumulation.[23] The computed glial interactome at the chronic active edge also comprises tissue-resident T cells and plasmablasts, reactive and inflamed astrocytes (with a signature partially overlapping neurotoxic astrocytes[24]), stressed oligodendrocytes and antigen-presenting oligodendrocyte precursor cells.[23]

Multiple astrocyte phenotypes have been identified in CAL. These phenotypes include: MAFG-driven astrocytes characterized by repressed antioxidant and anti-inflammatory transcriptional programmes[25] and adenosine receptor 2A positive astrocytes,[26] which exhibit reduced connectivity and reduced barrier function. Conversely, a regulatory astrocyte subpopulation has been found to be substantially reduced in acute and chronic active multiple sclerosis lesions. This subpopulation expresses the death receptor ligand TRAIL and limits CNS inflammation by inducing T cell apoptosis.[27]

Thus, CAL contain a multitude of reactive glial cell phenotypes, of which iron-containing microglia are only one subpopulation. The functional significance of these subpopulations in formation and maintenance of CAL in multiple sclerosis remains to be determined. Complement component C1q, which has multiple context-dependent roles in inflammation, has been recently shown to mediate activation of microglia and astrocytes in CAL.[23]

Many studies have highlighted large inter-individual variability in the frequency of different glial subpopulations.[20,21,28] Moreover, there is partial overlap with glial phenotypes described in other neurodegenerative diseases and disease models.[28,29]

Similarly, the descriptions of active, CAL and chronic inactive cortical lesions according to the distribution and density of MHC class II-positive cells have been reported in initial post-mortem examinations,[30] and in subsequent studies of either early[31,32] or progressive multiple sclerosis cases often in association with overlying leptomeningeal inflammation.[33]

Consensus statement on the *in vivo* imaging of chronic active lesions in multiple sclerosis

In vivo imaging of chronic active lesions in multiple sclerosis

Discussion

In recent years, the discovery of innovative MRI and PET-derived biomarkers has made it possible to detect, and to some extent quantify, CAL in the white matter, and to a lesser extent in the cortical grey matter, of patients with multiple sclerosis, *in vivo*. These newly identified biomarkers include: (i) PRLs on susceptibility-sensitive MRI sequences; (ii) MRI-defined SELs on T_1-weighted and T_2-weighted MRI sequences; and (iii) 18-kDa TSPO-positive lesions on PET. Presently, there are no MRI data supporting the visibility of SELs and CAL in the spinal cord, likely due to lack of suitable imaging technologies to detect these lesions in this anatomical area.

(1) PRLs are detected on susceptibility-sensitive MRI. PRLs display a T_2-hyperintense core that does not enhance with GBCA and is surrounded by a paramagnetic rim on susceptibility-sensitive MRI along at least two-thirds of the lesion perimeter (Fig. 1 and Box 1).

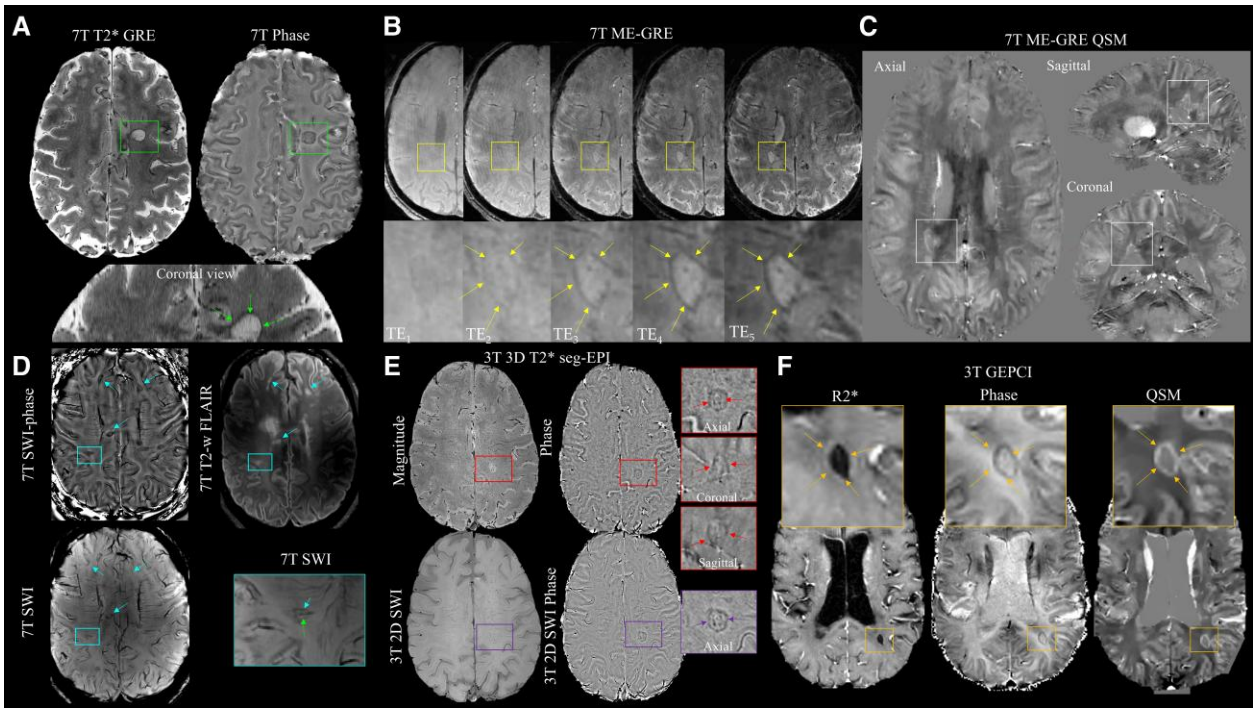

Figure 1 Paramagnetic rim lesion (PRL) visibility. (**A**) Axial and coronal slice of a PRL visible on a 7 T T_2*-weighted (T2*-w) single gradient echo MRI, magnitude and unwrapped filtered phase images with echo time = 32 ms, repetition time = 1300 ms, in-plane voxel size = 0.2 × 0.2 mm, slice thickness = 1 mm and scan time ~8 min. The hypointense rim signal (rectangles on the axial views, arrows on the coronal view) surrounds the hyperintense lesion core. Image contributed by Dr Martina Absinta, Dr Pascal Sati and Dr Daniel Reich. (**B**) Axial slices of a 7 T T_2*-weighted multi-echo GRE (ME-GRE) with flow compensation, magnitude images, echo time (TE) $TE_1/TE_2/TE_3/TE_4/TE_5$ = 5/10/15/20/25 ms, repetition time = 28 ms, in-plane voxel size = 0.65 × 0.65 mm, slice thickness = 0.7 mm, scan time ~ 8 min. It is important to highlight how PRL visibility (rectangles and arrows in the *insets*) increases with longer echo time. (**C**) Axial, sagittal and coronal views of a different PRL visible on quantitative susceptibility mapping (QSM) derived from the same sequence (rectangles). Here the hyperintense signal surrounds the lesion core, which is slightly hyperintense. Image contributed by Dr Seongjin Choi and Dr Daniel Harrison. (**D**) 3D susceptibility weighted imaging (SWI) and unwrapped filtered phase next to a T_2-weighted fluid attenuated inversion recovery (FLAIR) image at 7 T. 3D SWI pulse sequence parameters include echo time = 15 ms, repetition time = 50 ms, in-plane voxel size = 0.4 × 0.4 mm, slice thickness = 2 mm, scan time ~ 10 min. A few PRLs show that the hypointense rim surrounds the lesion core (compare with the FLAIR image) (arrows). An advantage of using SWI stems from its complementary ability to identify veins, allowing to: (i) distinguish PRL from curvilinear veins potentially mimicking a rim; and (ii) identify the central vein sign when needed. Shown in the *inset* is a PRL (arrow) transverse by a central vein (arrow). Image contributed by Habeeb F. Kazimuddin, Jiacheng Wang and Dr Francesca Bagnato. (**E**) The panel shows 3 T custom T_2*-weighted segmented 3D echo planar imaging (3D T2*-EPI) magnitude and unwrapped filtered phase images juxtaposed to vendor-provided multi-echo 2D SWI and unwrapped filtered phase images of the same lesion. Pulse sequence parameters include echo time = 27 ms, repetition time = 51 ms, isotropic voxel size = 0.55 mm, and scan time ~ 5 min for the 3D T2*-EPI, and $TE_1/TE_2/TE3/TE_4$ = 7.2/13.4/19.6/25.8 ms, repetition time = 31 ms, voxel size = 0.45 × 0.45 mm, thickness = 2 mm and scan time ~ 3 min for the 2D SWI. The isotropic voxel size and the T_2-weighting of the 3D T2*-EPI allows better visualization of the PRL on the three orthogonal planes (shown in the *inset*). Image contributed by Dr Martina Absinta. (**F**) Multi-echo gradient echo plural contrast imaging (GEPCI) allows for reconstructing R2*, unwrapped filtered phase and QSM at 3 T. Axial images are presented. The rim of the PRL has hyperintense signal on R2* and QSM and hypointense signal on the unwrapped phase. Pulse sequence parameters here include 10 echo times, with the first = 4 ms and echo spacing of 4 ms, repetition time = 40 ms, in-plane voxel size = 1 × 1 mm, slice thickness = 2 mm, scan time = 12 min. Image contributed by Dr Biao Xiang, Dr Dimitriy Yablonskiy and Dr Anne Cross.

(2) SELs are derived from conventional MRI, representing areas of pre-existing T_2 lesions that show slow, constant, gradual and radial expansion over T_1-weighted and/or T_2-weighted MRIs acquired longitudinally over time (Fig. 2).
(3) TSPO-positive lesions are defined as those areas that co-localize to a hyperintense core on a T_2-weighted image, do not enhance with GBCA on T_1-weighted MRI and demonstrate an increased uptake of TSPO in the border, on PET (Fig. 3).

Statements and recommendations

PRLs, SELs and TSPO-positive lesions are candidate biomarkers of CAL.

Knowledge gap

It remains to be established definitively: (i) how SELs on T_1-weighted and T_2-weighted MRI, and TSPO-positive lesions on PET, relate to PRLs and CAL; and (ii) which of the three biomarkers is most specific for and sensitive to CAL.

Histopathologic validation of paramagnetic rim lesions in the white matter

Discussion

Combined MRI-histology studies provide histopathological validation of PRLs in the brain white matter seen on gradient echo (GRE)-derived R2*/T_2* maps,[37–39] quantitative susceptibility maps (QSM),[40–43] phase images[37,38,44–48] and susceptibility-weighted imaging (SWI) (Fig. 4).[49,50]

At the time of drafting this manuscript, histopathological characterization of 73 PRLs and 76 non-PRLs has been reported by four independent laboratories in 24 cases with multiple sclerosis (Supplementary Table 1).[37,40–47,49,50] The highly concordant data

Box 1 Radiological definition of a white matter paramagnetic rim lesion

Features of the paramagnetic rim lesion (PRL) rim

- A discrete rim with paramagnetic properties on a susceptibility-sensitive MRI sequence at ≥1.5 T that is continuous through at least two-thirds of the outer edge of the white matter portion of the lesion (excluding any cortical or ependymal border), on the slice of maximum visibility (Fig. 1).
- The rim co-localizes with the edge of all or part of a lesion core that is hyperintense on T_2-weighted images; in case of large T_2-lesions, the detection of the PRL core can be facilitated by also looking at a more discernible hypointense core on T_1-weighted images (Fig. 6).[a]
- The rim (or part of it) is discernible on at least two consecutive slices (2D acquisition) or in two orthogonal planes (3D acquisition).

Features of the PRL core

- Co-localizes with all or part of a T_2-hyperintense lesion that does not enhance on T_1-weighted post-gadolinium-based contrast agent (GBCA) images.[b]

Exclusion criteria

- Veins running alongside the rim that may resemble a rim.

Red flags and cautions (not necessarily ruling out the classification of a lesion as PRL)

- Small paramagnetic/diamagnetic structures, e.g. iron-laden ferritin or hemosiderin dots, veins and myelin debris. However, such features may also accompany a true rim.
- Small PRL core (e.g. diameter <3 mm in greatest dimension)
- Rim thickness >2 mm (for phase maps especially, when the susceptibility changes seen inside the lesion core cannot be distinguished from those seen in the rim).
- Lesions showing magnetic dipole artefacts (often best seen in coronal or sagittal reformations).
- Anatomical regions with susceptibility artefacts (much of the anterior temporal lobes, orbitofrontal cortices and infratentorial brain).
- Challenges in reaching an agreement in the determination of a PRL.

[a]Confluent lesions are not excluded from the PRL determination if a reasonable attempt to discern an embedded PRL surrounding a distinct core can be made.
[b]If post-GBCA MRI is not available, a PRL should only be defined as such when the corresponding lesion was present on a T_2-weighted scan acquired at least 3 months (ideally 6 months) prior. If both post-GBCA MRI and such a prior scan are not available, a PRL should be marked as 'possible', and its chronicity should be confirmed with a scan acquired at least 3 months (ideally 6 months) later. The 6-month window is based on established literature demonstrating that enhancement of an acute white matter lesion very rarely exceeds 6 months.[34–36]

show that the core of PRLs has near complete loss of myelin. The rim of PRLs co-localizes with the presence of ferritin-bound iron, which is prevalently located inside CD68+ cells, most of which are likely of microglial origin (Fig. 4). Cumulatively, these features indicate that PRLs correspond to CAL as traditionally defined histopathologically. This statement is further corroborated by the demonstration that PRLs seen on post-mortem samples can correspond to lesions that expanded *in vivo* preceding death.[44,45]

The specificity and sensitivity of MRI to PRLs has not been systematically analysed. Lack of these data is largely due to the relatively small number of cases available and analysed thus far in individual centres. With respect to MRI specificity, only one study has identified a low rate[43] of false-positive PRLs (PRL identified by MRI without the expected histology counterpart) or false-negative CAL (positive histology without MRI corroboration). Specifically, using QSM maps, the authors reported that 39 of the 42 identified PRLs (93%) corresponded to CAL and three to chronic inactive lesions. Regarding MRI sensitivity, the same authors reported that 37/40 (93%) CAL by histopathology corresponded to a PRL, and the remaining three CAL were diffusely hyperintense on QSM.[43] Notwithstanding this consideration, it is important to note that while iron-laden cells can be invariably present at the edge or in the centre of several multiple sclerosis lesion subtypes, their quantity is far larger in the rim of PRLs relative to other lesions and non-lesional sites.[42,44,49] This factor is responsible for their unique visibility on MRI.[49] For the same reason, the rim may not always appear to surround the lesion core in its entirety. Similarly, microglia may be present also outside the rim of CAL, e.g. both within the lesion core and in the normal-appearing white matter beyond the rim.[11] However, the absence of iron inside these microglia makes them invisible to MRI.

Statements and recommendations

(1) Highly concordant and independent evidence supports the notion that PRLs on MRI correspond to CAL.
(2) The amount of iron+ cells is a major determinant of PRL visibility on susceptibility-sensitive MRI.

Knowledge gap

Combined imaging-histopathology studies based upon large sample cohorts are needed to: (i) measure the sensitivity of PRLs to identify all (or nearly all) CAL in brains of patients with multiple sclerosis and assess the source of false-positive and false-negative findings; (ii) identify and characterize radiological features of PRLs that can relate to the presence or absence of ongoing demyelination; (iii) assess whether the presence of PRLs is indicative of other MRI and histological features of microglia-driven chronic inflammation and demyelination elsewhere in the brain; (iv) identify radiological features indicative of the stage of CAL; and (v) characterize the degree of axonal injury within CAL.

MRI acquisition and postprocessing methods for the detection of paramagnetic rim lesions in the white matter

Discussion

Several susceptibility-sensitive MRI acquisition and postprocessing methods have been proposed to characterize and detect PRLs.

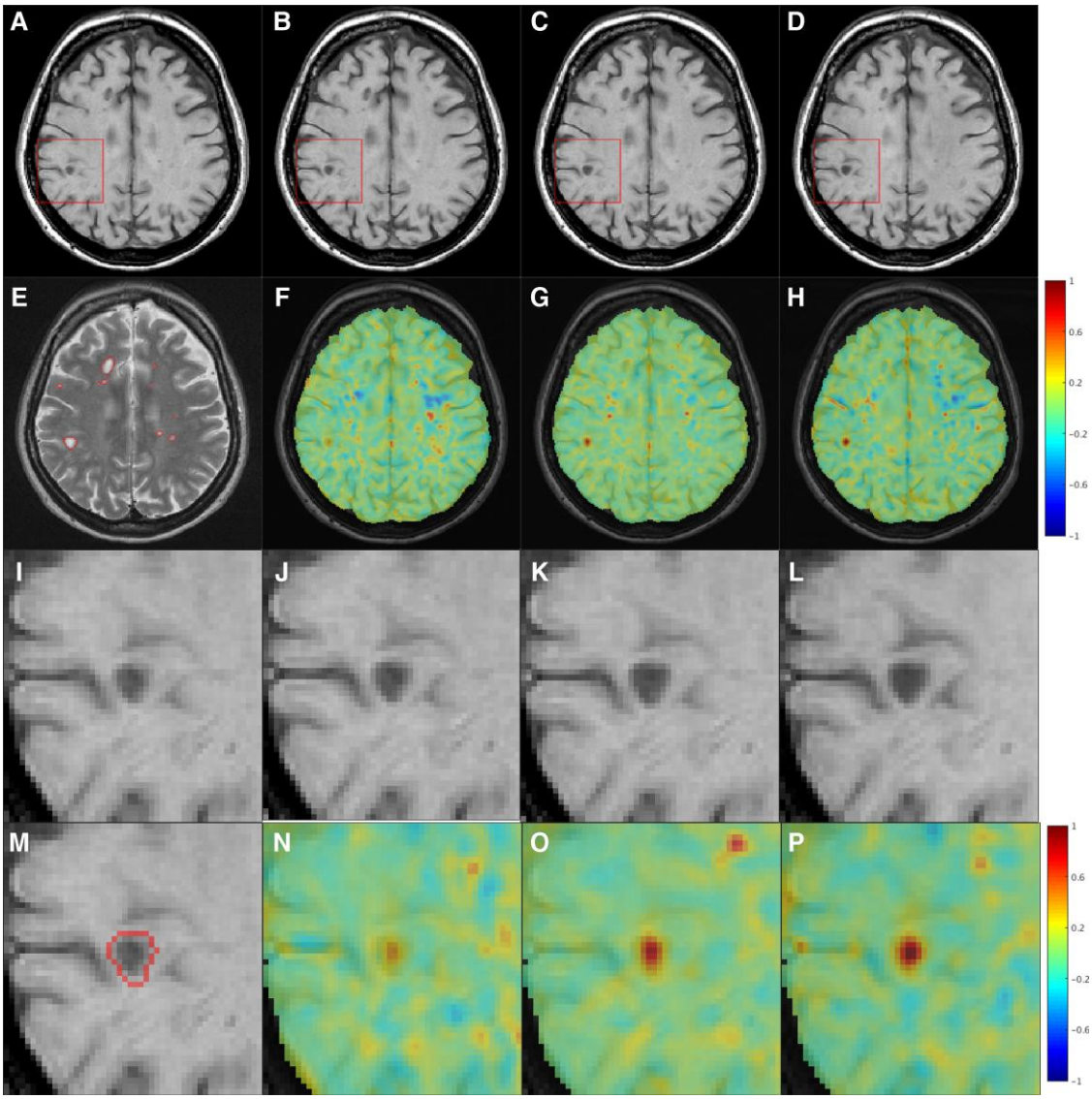

Figure 2 MRI-defined slowly expanding lesions (SELs). (**A**) Axial slice of T_1-weighted MRI at baseline; (**B**) 6 months; (**C**) 12 months; (**D**) and 24 months; and (**E**) T_2-lesion mask of baseline scan. (**F**) Jacobian determinant maps at 6 months, (**G**) 12 months and (**H**) 24 months, all with respect to baseline, where values >0 (red) indicate expansion and values <0 (blue) indicate shrinkage. A region of interest corresponding to red box in **A**–**D**, at baseline (**I**), 6 months (**J**), 12 months (**K**) and 24 months (**L**). In **M** the lesion area, identified as SEL, is contoured. Jacobian determinant maps in region of interest at 6 months (**N**), 12 months (**O**), 24 months (**P**), all with respect to baseline, showing the gradual expansion over time. Image contributed by Dr Colm Elliott.

Initial studies used T_2*-weighted single echo GRE[45,49] or multi-echo GRE (ME-GRE)[38,51–54] scans at 7 T. Susceptibility effects increase with magnet field strength, and the combination of greater effects with higher signal-to-noise/contrast-to-noise ratios leveraged for higher spatial resolution scans provide support that 7 T MRI is the current gold standard for PRL comparisons with lower magnetic field MRI acquisitions.

Seven-tesla imaging has provided the benchmark for numerous studies at 3 T and 1.5 T, which are more accessible for routine evaluation. An example of these efforts is the implementation of faster isotropic 3D GRE/ME-GRE scans with shorter repetition time. Such methods improve signal sensitivity but result in significant T_1-weighting.[55] A reduction in the number of slices covering the brain has also been pursued, resulting in thicker slices and reduced sensitivity to smaller lesions.[56–61] As a compromise between these two approaches, a segmented (multi-shot) EPI method has been implemented.[62] This method allows submillimetre isotropic resolution while preserving and enhancing T_2*-weighted contrast at 3 T.[46,63–66] The use of submillimetre isotropic resolution is particularly useful for facilitating the identification of PRLs in two or more orthogonal viewing planes.[63]

The different types of GRE-based acquisitions can provide both magnitude and phase images, which, in combination, can be postprocessed to enhance the visibility of PRLs. Examples of different postprocessing methods include SWI,[67] susceptibility-weighted angiography (SWAN) and SWI-phase (SWIp), all three of which provide different vendor-supported combinations of magnitude and phase information that use proprietary algorithms. Relying solely on phase information by applying two-step postprocessing (phase unwrapping[68–71] followed by phase filtering[71–74]) provides a vendor-agnostic sensitivity-enhancement approach. This latter approach is very sensitive to PRLs but suffers the main disadvantage of

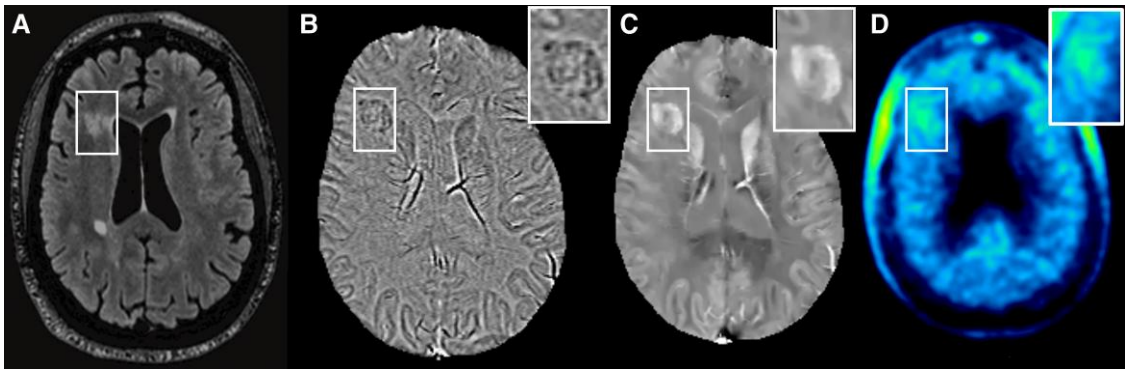

Figure 3 Increased uptake of 18-kDa translocator protein (TSPO) on PK11195 PET in a paramagnetic rim lesion. (**A**) Hyperintense lesion on T_2-weighted FLAIR image identified within the rectangle in a person with relapsing-remitting multiple sclerosis. The lesion is a paramagnetic rim lesion (PRL), as seen on the unwrapped filtered phase image (**B**, *inset*) and quantitative susceptibility map (**C**, *inset*). It has corresponding high TSPO uptake on PK11195-PET (**D**, *inset*). Image contributed by Dr Ulrike Kaunzner, Dr Thanh Nguyen and Dr Yeona Kang. FLAIR = fluid attenuated inversion recovery.

featuring dipolar artefacts caused by the geometry and orientation of veins and lesions, possibly resulting in the appearance of 'pseudo-PRLs'.[74,75] We expand on the nature of this phenomena in Supplementary Fig. 1.

QSM is a possible solution to the 'pseudo-rim lesions' challenge because it can effectively remove dipolar artefacts from veins and lesions.[76,77] However, QSM requires solving the phase-to-susceptibility inversion, which is an ill-posed mathematical problem[76] for which many solutions have been proposed.[77–83] Furthermore, QSM images can feature streaking artefacts and noise amplification with detrimental effects on image interpretation that have not yet been fully analysed.

Finally, T_2^* relaxometry, which uses the signal magnitude as a function of echo time from ME-GRE scans, has been proposed to visualize and quantify the R_2^* ($=1/T_2^*$) relaxation rate constant, which is strongly affected by the iron accumulation in the paramagnetic rims.[38,51,84,85]

Given the multitude of contrasts proposed for imaging PRLs, it is important to remember that the signal intensity of the rim (hypo- or hyperintense depending on the convention used for image reconstruction) should always indicate a paramagnetic effect. Thus, the rim signal should always match with the signal intensity of veins, which contain paramagnetic deoxyhaemoglobin. Importantly, there is no universally accepted convention for display of phase images, so paramagnetic rims may appear either hypointense or hyperintense relative to white matter depending on the convention chosen.

Clinical studies in multiple sclerosis have tested the ability of most of the proposed methods to detect PRLs at 1.5 T, 3 T and 7 T although a few studies only compared PRL visibility across field strengths[86] or imaging methods.[87] Given the lower signal-to-noise and contrast-to-noise ratios at 1.5 T, technical studies optimizing the detection of PRLs at 1.5 T are needed. No formal comparisons have also been performed between 3D and 2D acquisitions. While 3D acquisition is preferred due to its ability to provide thinner slices and more efficient scanning speed, 2D acquisition remains feasible if the slice thickness is kept at 3 mm or less. Comparative studies are also needed to establish how all available methods compare to one another in terms of feasibility, sensitivity, specificity and reliability, all of which are important factors for clinical translation. It is possible that each method may have its unique applicability. Vendor-supported SWI or phase images may be of easier widespread clinical implementation while techniques requiring more sophisticated postprocessing, like QSM, may be more suitable for research studies.

Finally, there are currently no published studies assessing the effect of GBCA on visualization of PRLs.

Statements and recommendations

(1) PRLs can be visualized at 1.5 T, 3 T and 7 T.
(2) Given the increase in magnetic susceptibility effects at higher magnetic field strengths, and the fact that paramagnetic rims are commonly thin, the suggested acceptable standard for visualization of PRLs is ≥1.5 T MRI with submillimetre in-plane and ≤3-mm through-plane resolution for 2D acquisitions, ≤2-mm or higher resolution isotropic for 3D ones.
(3) Post-acquisition processing of magnitude and phase images and multiplanar viewing are required for proper identification of PRLs. Processing options include SWI, R_2^* relaxometry, unwrapped/filtered phase and QSM. Each method has advantages and disadvantages.

Knowledge gap

Multicentre studies based on large sample cohorts are needed to compare the accuracy of each acquisition and postprocessing method for identifying PRLs in patients with multiple sclerosis, using 1.5 T, 3 T and 7 T scanners and different through-plane resolutions.

Identifying and reporting white matter paramagnetic rim lesions

Discussion

Although MRI sequences sensitive to PRLs are widely available, they are uncommonly used for routine clinical imaging in multiple sclerosis. Currently, the next logical step is to foster efforts to incorporate PRL assessment into day-to-day clinical operations. To facilitate such effort, the panel proposed the importance of establishing criteria to routinely identify and report PRLs on MRI scans of patients with multiple sclerosis. Given that PRLs are a relatively new biomarker, the identification of which may be subjective, the panel proposed stringent criteria for their radiological definition, prioritizing the minimization of false-positive findings. To this end, it was advised that until the assessment of PRLs becomes standard of care, radiologists seek *ad hoc* training in specialized centres or with experienced investigators as they start to identify PRLs in day-to-day clinical practice. We detail identification criteria for PRLs along with proposed ways to report their presence and

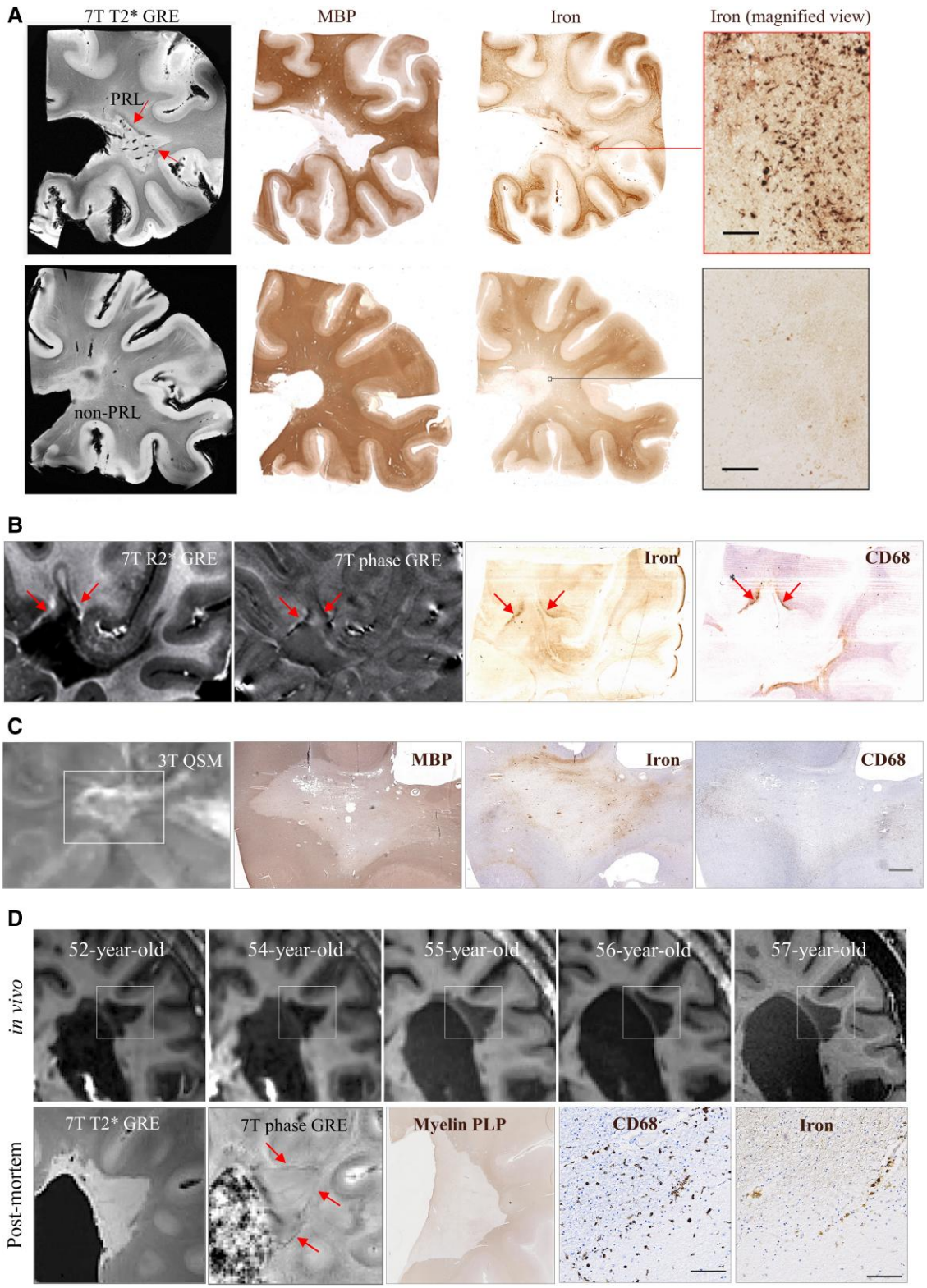

Figure 4 Histopathological validation of paramagnetic rim lesions using different acquisition and postprocessing MRI methods. (**A**) A paramagnetic rim lesion (PRL) is seen on a multi-echo gradient echo (ME-GRE) T_2^* image at 7 T. The paramagnetic rim (arrow) partially surrounds a demyelinated lesion core [absence of myelin basic protein (MBP) stain] and co-localizes with peripheral intracellular iron (low and high magnification views). The lesion in the second row is not a PRL and has no iron rim. Similar findings are presented in **B** and **C**, where PRL are shown on ME-GRE R2* and phase image at 7 T and quantitative susceptibility imaging (QSM) at 3 T. In **B**–**D**, iron co-localizes with CD68+ activated macrophages/microglia. In **D**, *in vivo* MRI shows that this PRL slowly enlarged over the course of 5 years prior to death. Image contributed by Drs Simon Hemetner and Assunta Dal Bianco (**A**) Drs Simon Hemetner, Bing Yao and Francesca Bagnato (**B**), Dr Susan Gauthier (**C**) and Drs Martina Absinta and Daniel Reich (**D**).

Box 2 Features relevant to paramagnetic rim lesion reporting

Desirable features useful in both clinical and research settings

- Indicate the MRI sequence and postprocessing method used to identify PRL (Box 1).
- Indicate the number of PRLs (ideally, exact count to 10, or >10).
- PRLs may be qualified as 'possible' based on the availability of a post-contrast scan (Box 1).
- Indicate qualitative PRL changes, if any, in comparison to prior scans: (i) lesion size (stability, shrinkage or enlargement); (ii) paramagnetic rim (changes in extent of lesion coverage or intensity, including disappearance).[a]

Optional features useful in research settings

- Indicate the analysed field of view, e.g. above the tentorium.
- Indicate location of PRL, e.g. periventricular, deep white matter, juxtacortical, cortical.
- Indicate if a PRL co-localizes with a distinct lesion on T_2-weighted MRI versus part of a confluent large lesion.

[a]Note that such changes may take several years to become evident, so comparison to older prior scans should be made when possible.

features in Box 1 and Box 2 and present here the four major points of discussion along with challenges related to PRL identification.

Accurately establishing lack of acute activity

The panel suggested making every effort to ensure lack of radiological signs of overt acute inflammatory activity, especially visually apparent GBCA enhancement, at the site of a PRL. This proposition stems from the notion that PRLs are chronic lesions. Acute GBCA-enhancing lesions, particularly those with a 'rim' or 'centripetal' enhancement pattern, may exhibit susceptibility effects at the locus of GBCA enhancement that mimic those seen in PRLs.[48] This finding may disappear upon resolution of enhancement,[44,51] and PRLs indicative of CAL are only those that persist thereafter (Fig. 5). Thus, the identification of PRLs should include a concomitant or any prior T_1-weighted post-GBCA scan to confirm that the identified lesion does not feature GBCA enhancement. If a post-GBCA MRI is not available, a PRL should only be definitively identified when the corresponding lesion core was present on a T_2-weighted scan acquired at least three (ideally six) months prior. If both post-GBCA MRI and at least 3-month (ideally six) prior scan are not available, a PRL should be defined as 'possible', and its chronicity should be confirmed with a scan acquired ideally at least 3 months (ideally six). The 6-month window is based upon established literature demonstrating that persistent GBCA enhancement after 6 months is exceedingly rare.[34–36]

Challenges in the detection and delineation of paramagnetic rim lesions

Two main challenges were recognized as important when identifying PRLs. First, the panel discussed difficulties with the delineation of PRLs when this is part of a larger lesion that was likely generated by confluency of several discrete inflammatory events. The panel recommended counting any reasonably discernible PRLs after detailing criteria for their identification and segmentation (Figs 1 and 6). Second, the panel recommended cautious interpretation of data derived from infratentorial brain regions given those areas' vulnerability to susceptibility artefacts related to magnetic field inhomogeneities.

Detecting and reporting changes in paramagnetic rim lesions over time

The panel discussed the importance of reporting comparisons of PRL visibility across scans over time. While more sophisticated quantification can be done in research settings, qualitative descriptions of detected changes can suffice in day-to-day clinical practice and potentially in reader-based clinical trials. Specifically, any appreciable change in lesion size (e.g. shrinkage or enlargement) and rim characteristics (e.g. extent of lesion core coverage, intensity changes or disappearance) should be noted. The panel also noted that at times the identification of a PRL may be debatable, given variable degrees of signal intensity and rim length (both ultimately likely linked to the PRL stage). Part of this challenge is also present on histology samples as the rim of microglia not always surround the lesion core on its entirety and/or is dependent on the iron quantity (as discussed earlier). *In vivo*, longitudinal assessments may often in time provide a clear understanding of certain lesions features. In recognition of this challenge, the panel suggested the possibility of qualifying PRLs as definite, probable or possible based on the degree of confidence.

Proposing a stringent criterion to define paramagnetic rim lesions

Given that the proposed effort represents the first attempt to standardize a radiological definition of PRLs, the panel agreed on the importance of a stringent initial criterion for the definition of PRLs, based on the presence of a rim perimeter surrounding the lesion core of at least two-thirds (Box 1). A discussion was held on the possibility that this criterion may in future prove to be not applicable to all MRI methods or to be unnecessarily stringent. However, the consensus was to start with a methodology that would minimize false-positive results.

Statements and recommendations

(1) Box 1 details the proposed criteria for the definition of PRLs on MRI.
(2) Box 2 details the proposed criteria for describing PRLs on a radiological report.

Knowledge gap

Investigations are needed to: (i) establish how the proposed PRL definition will perform in the multicentre setting as well as in comparisons with other proposed definitions (e.g. complete lesion perimeter only or 50% lesion perimeter); (ii) determine how to quantify clinically and biologically meaningful PRL changes over time; (iii) assess the proposed definition against histopathology; and (iv) compare PRL visibility across clinical centres using different available susceptibility-sensitive MRI techniques.

Automated detection of paramagnetic rim lesions in the white matter

Discussion

Expert visual assessment of PRLs is the gold standard for determining their presence. However, this approach is time-consuming and

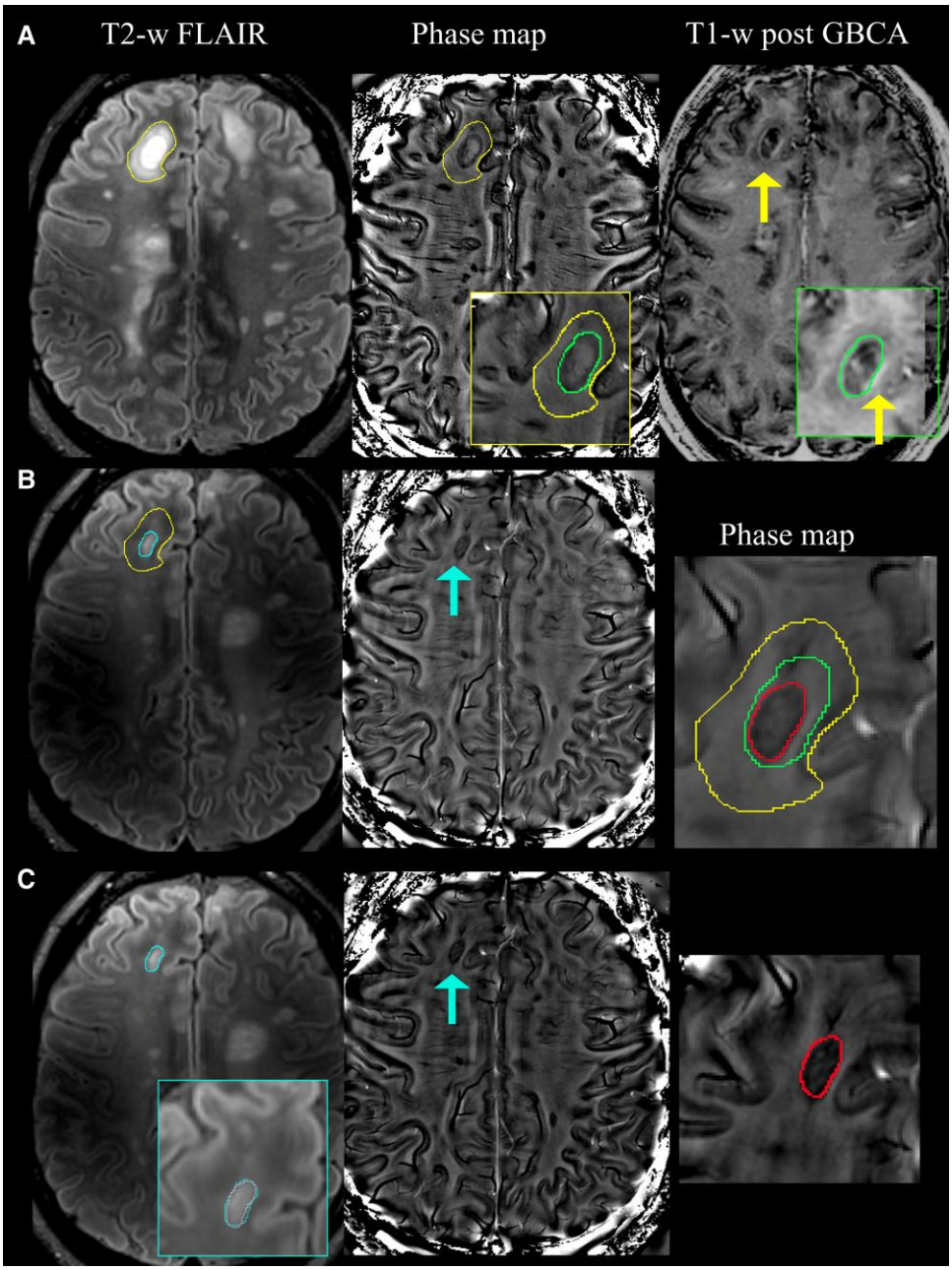

Figure 5 Paramagnetic rim lesion persisting upon resolution of gadolinium-based contrast enhancement. (**A**) T_2-weighted fluid attenuated inversion recovery (T_2-w FLAIR) image at 7 T showing a hyperintense lesion delineated by the yellow contour. The central more hyperintense core of the lesion is surrounded by a paramagnetic rim, as seen on the phase map presented next. There is likely vasogenic oedema (T_2-hyperintense signal) peripheral to the paramagnetic rim (green contour). The lesion also has gadolinium enhancement [yellow arrows on the T_1-weighted post-gadolinium-based contrast agent (GBCA) MRI], which co-localizes with the rim. Co-localization is shown with a green contour in the insets of the phase and T_1-weighted post-GBCA MRI. Note that on this scan, the lesion cannot be called a paramagnetic rim lesion (PRL) because it demonstrates contrast enhancement. (**B**) A year later, there is partial resolution of the previous large lesion on T_2-weighted FLAIR, now limited to the core area contoured in light blue (larger magnification in the *middle inset*). The lesion is no longer contrast-enhancing (data not shown) but retains PRL visibility on the phase map (indicated by the light blue arrow). The contour of the new phase rim is delineated in red, and it is contrasted with the size of the rim measured at baseline (green) and the overall lesion size at baseline (yellow). At this time point, the lesion can be called a PRL because it is no longer GBCA-enhancing and the paramagnetic rim (light blue arrow on phase map) co-localizes with the perimeter of the chronic lesion core (light blue) on T_2-weighted FLAIR. (**C**) At Year 2, the lesion has remained approximately of the same size as delineated by the purple contour (which nearly overlaps with the light blue one, refer to the T_2-weighted FLAIR *inset*). The PRL (light blue arrow on phase map) is also the same size (the red contour from Year 1 scan entirely overlaps with the rim on Year 2 scan, *inset*). Images were acquired on a person with newly diagnosed multiple sclerosis who was treatment naïve at the time of the baseline scan. Image contributed by Dr Francesca Bagnato, Habeeb F. Kazimuddin and Jiacheng Wang.

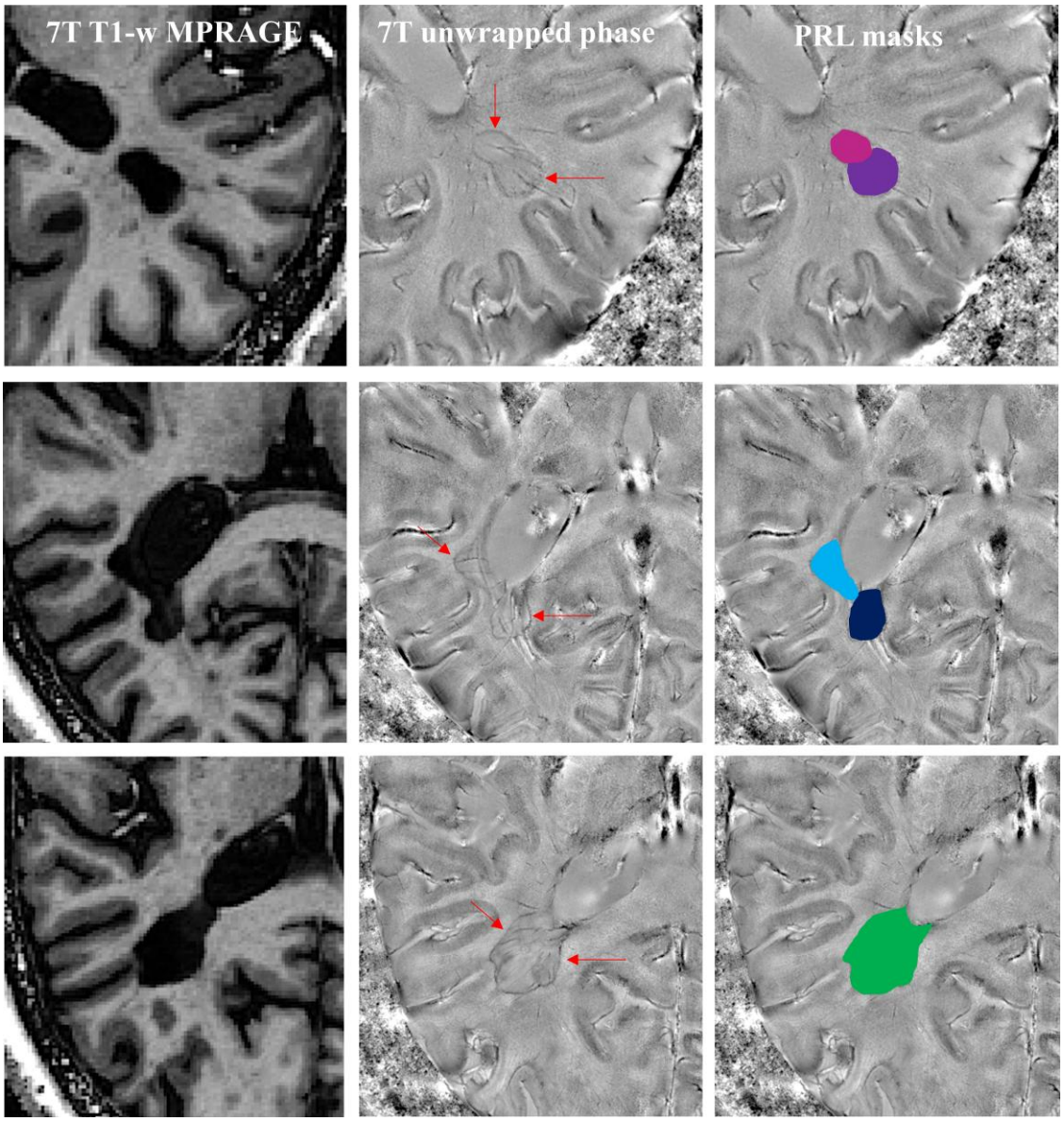

Figure 6 Paramagnetic rim lesion identification in the setting of large, confluent lesions. Representative examples of paramagnetic rim lesions (PRLs) and their suggested identification and segmentation (colour-coded PRL masks) in the setting of large, confluent lesions. In the first two cases, although the lesions are confluent on the T_1-weighted image, two PRLs can be clearly distinguished on the unwrapped filtered phase image. In the third case, a reliable PRL sub-segmentation is not achievable and the lesion should be counted as a single PRL (even though it may in fact represent the confluence of several PRL). Image contributed by Dr Martina Absinta and Dr Daniel Reich.

can be challenging. Methods for automated assessment of PRLs based on machine learning have recently been developed.[88,89] A deep learning-based method[88] used automated lesion segmentation[90] followed by manual correction and confluent lesion sub-segmentation to extract 3D patches around lesions. When integrating T_2-weighted fluid attenuated inversion recovery (FLAIR) and T_2^* phase imaging using a convolutional neural network approach, excellent classification performance was achieved. A contemporaneously developed method[89] employed a fully automated statistical approach for PRL detection. This method used automated lesion segmentation[91,92] followed by automated confluence removal[93] and extraction of radiomic features[94] from each lesion. A random forest classifier then achieved good performance. Further developments in the field continue, including those employing QSM[95] for rim detection.

Statements and recommendations

(1) The current gold standard for PRL identification and quantification is visual review by trained experts.
(2) Preliminary data suggest that automated algorithms hold promise for PRL detection, but further validation is necessary.

Knowledge gap

Further studies are needed to develop automated algorithms for detecting PRLs, quantifying PRL features (e.g. core volume, rim intensity, and rim extension) as well as their changes over time.

White matter paramagnetic rim lesions for multiple sclerosis diagnosis and prognostication

Discussion

Prior to discussing the role of PRL for disease diagnosis and prognosis, the panel highlighted three specific features of PRLs, potentially affecting clinical-MRI correlative studies.

First, PRLs have been observed to arise at the time of lesion formation.[44,48,51,96–99] In studies that assessed both susceptibility and GBCA-enhancement simultaneously, one found that 41% of all GBCA-enhancing lesions showed a QSM+ rim[97]; two other studies observed that 34%[99] and 52%[44] showed a phase rim at the time of enhancement. In a follow-up period of 6+ months, QSM+ rims persisted, with an additional 3%[99]–9%[97] of lesions evolving to include a newly observed rim at some point; whereas phase rims were observed to disappear in 5%[99] and 45%[44] of initially rim+ lesions at 3–6 months follow-up. The initial (non-susceptibility) MRI feature that appears to most consistently predict formation of a persistent PRLs include larger lesion size.[44,96,97,99] Other features of probable importance include a ring[44,97,99] (centripetal[44])-enhancing pattern, longer T_1 prolongation[99] and a transient hypointense rim on apparent diffusion coefficient maps.[96] For example, across two studies that reported the enhancement pattern of 131 lesions, 66% of GBCA-ring-enhancing lesions developed persistent PRLs, compared to only 5% of GBCA-nodular-enhancing lesions.[44,96] Thus far, chronic T_2-lesions have not been reported to evolve into PRLs over time, although studies based on numerous serial post-GBCA MRIs would be required to more fully assess this.

Second, studies have shown that PRLs have features of more aggressive pathology but not blood–brain barrier injury[100] relative to rimless lesions and, as such, may have a negative effect on outcome. Specifically, PRLs are larger than rimless lesions,[44,49,50] also at the time of the GBCA-enhancement[48,97,99] and tend to remain stable or enlarge longitudinally,[45,49,50,98,101,102] whereas rimless lesions tend to remain stable or shrink.[45,49,50,98,101] PRLs were seen to be invariably hypointense on T_1-weighted gradient echo sequences[45,50,103,104] and demonstrate greater underlying tissue injury, as measured using quantitative MRI methods, compared to rimless lesions.[45,50,100,104–107] Nonetheless, as many as 56% of PRLs were found to correspond to a black hole, as traditionally defined on T_1-weighted spin echo images,[51] highlighting the fact that, at each given time, PRLs do not necessarily represent all lesions with the highest degree of tissue loss in brain. Furthermore, periplaque damage around PRLs seems to be worse than around rimless lesions.[105] In light of these findings, the association between PRL status (≥1) or number and higher (group-level) T_2-hyperintense lesion volumes is a potential confound for cross-sectional interpretation. Thus, both the total T_2-lesion burden as well as PRL status/number should be considered as covariates when performing clinical correlative studies.

Third, in a fraction of PRLs, still not consistently estimated, the T_2-hyperintense core persists while the paramagnetic rim fades over time; this leads to apparent resolution of the PRL. Studies have shown that it may take up to 3.5 years to see PRLs enlarging[49] and a median of 7 years[23] to notice their resolution. Whole-lesion QSM decay begins ~1.5 years for rimless lesions whilst susceptibility remains elevated from PRLs up to 4 years of age.[97] This dynamic behaviour of PRLs affects the output of clinical-MRI correlative studies, in that lesions that were formerly PRLs but are still associated with disability would then be counted as rimless lesions in cross-sectional studies.

The role of paramagnetic rim lesions in distinguishing multiple sclerosis from mimickers

At the time this paper was drafted, 11 adult studies[52,58,59,64,108–114] had been published assessing the role of PRL in distinguishing multiple sclerosis ($n = 968$) versus incidental lesions in heathy controls ($n = 299$) or multiple sclerosis-mimicking diagnoses ranging from infectious, inflammatory, autoimmune, vascular and non-inflammatory aetiologies ($n = 297$). They reported a consistently high (>90%) specificity for PRLs to discriminate multiple sclerosis from mimics,[52,58,59,108–114] except for Susac's syndrome, in which PRLs are seen in ~60% of cases.[59,64,111] Notably, however, the number of Susac's syndrome cases in these studies is low (11 individuals). In contrast, the sensitivity of PRLs in multiple sclerosis diagnosis remains modest at best, ranging from 24% to 52% in the largest cohorts.[64,112] Of additional diagnostic relevance, one study noted that in cases of clinically isolated syndrome, 100% of those having >1 PRL at baseline were ascertained as having relapsing multiple sclerosis over a 4.5-year follow-up period.[59] A primary limitation of these studies is the relatively modest sample size.[59]

Paramagnetic rim lesions as indicators of worse clinical, radiological and biological outcome

The panel acknowledged that PRLs have been observed across all multiple sclerosis clinical phenotypes and radiologically isolated syndrome.[115,116] Studies indicate that the prevalence rates mostly range around 50%–60% when assessed using a consistent 3 T protocol.[64] While numerous studies have been performed to report on the occurrence of PRLs, the discussion relative to clinical-MRI correlative outputs generally focused on studies examining multiple clinical status measures with larger ($n > 50$) sample sizes.

Most of these cross-sectional studies showed an association between PRLs and higher physical[45,61,64,117] and cognitive[44,117] disability. A few did not.[66,118] No study identified a protective association with PRLs. Cross-sectional cohorts also revealed associations between PRLs and lower grey matter volumes,[45,61,103,115,117] cortical thickness,[117] cortical lesions[102] and whole brain volumes,[45,115] as well as greater spinal cord lesion burden and atrophy.[61]

A predilection for PRL anatomical localization in periventricular areas has been reported thus far[119,120] although findings are not unequivocal.[121] Comparisons in network dysfunction between PRL+ and PRL– patients with multiple sclerosis found less network disruption in the former group, indicating that the effect of PRLs on disability is not mediated by it but also raising the question on the remote impact of PRLs.[121,122]

Finally, PRLs have recently been shown to have an association with CSF chitinase-3-like-1 protein (a marker for microglial activation),[118] a higher intrathecal immunoglobulin G (IgG) synthesis,[123] as well as increased albumin quotient[103] and serum neurofilament light chain, in most[46,118,124] but not all studies.[101] The correlation between PRLs and haemolysis parameters, previously found to be associated with features of neurodegeneration,[125] was non-significant.[126] The studied haemolysis, haematologic and blood chemistry parameters included red blood cell count, reticulocytes, haemoglobin, haematocrit, potassium, iron, total bilirubin, free haemoglobin, haemolysis index, lactate dehydrogenase, fibrinogen and aspartate transaminase levels.[126]

In contrast to cross-sectional studies, longitudinal disability data are scarce. Three independent groups[102,104,127] conducted prospective

assessments ($n = 100$, $n = 66$, $n = 91$); even after adjusting for baseline lesion volume, all observed that the baseline number of PRLs—but not necessarily PRL status (presence/absence)—predicted worsening disability or conversion to secondary progressive multiple sclerosis (SPMS) [but not clinically isolated syndrome (CIS) to relapsing remitting multiple sclerosis (RRMS)] over a follow-up period up to 9 years.[127] Other recent retrospective studies ($n = 61$ and $n = 72$) also found longitudinal disability worsening associated with ≥1 PRL (over a median 3.2 years),[128] or ≥4 PRLs (over a median ∼2 years).[129]

It is to be highlighted, however, that a high degree of methodological inter-study variability is present due to differences in MRI postprocessing, hardware and software acquisition parameters, image analysis techniques and statistical design/interpretation. These factors challenge the validity of comparisons among cohorts.

Statements and recommendations

(1) PRLs likely develop in the wake of newly formed T_2-lesions and persist for several years.
(2) Over time, PRLs may enlarge and the paramagnetic rims may persist or fade.
(3) PRLs can be seen at any stage of multiple sclerosis as well as in radiologically isolated syndrome, but they are often associated with a more aggressive clinical and radiological course.
(4) The high specificity of PRLs for multiple sclerosis suggests that they could prove useful as a supportive MRI feature for the diagnosis of multiple sclerosis.

Knowledge gap

Although a highly promising biomarker, the establishment of the role of PRLs as clinical biomarker warrants further investigations. Studies are needed to determine: (i) the prevalence of PRLs in each disease phenotype and the consistency of such prevalence across different MRI protocols; (ii) the role of PRLs as prognostic biomarkers of disability accumulation in large, prospective longitudinal studies; (iii) the role of disease-modifying agents, environmental variables and genetic features on PRL formation/evolution; (iv) the clinical impact of preventing and/or resolving PRLs; (v) how different methodological approaches impact clinical-radiological correlations; and (vi) the GBCA-enhancing and T_2-weighted lesion features that predict PRL development.

Paramagnetic rim lesions in the cortical grey matter

Discussion

Although studies focused on the identification of PRLs in the cortex of patients with multiple sclerosis are limited,[8,102,130–132] *in vivo* examinations at 7 T report that some leukocortical multiple sclerosis lesions feature a paramagnetic rim.[8,102,130] Cortical PRLs identified on GRE-derived T_2^* and QSM have both been validated against histology as CAL. QSM maps alone, however, cannot distinguish susceptibility contributions of demyelination and iron increase. For this purpose, future studies could combine information from both QSM and R2*/T2* mapping or use susceptibility separation techniques.[132] QSM reconstruction techniques are not yet completely optimized for the cortex, so a variable proportion of cortical lesions could be missed.

PET imaging based on targeting 18 kDa mitochondrial TSPO expression, a marker of glial activation, has provided *in vivo* evidence of neuroinflammatory activity within the cortex[133,134] and cortical lesions[135] of patients with multiple sclerosis. Initial data demonstrate that TSPO PET imaging could be helpful for staging cortical lesion inflammatory activity *in vivo* in a manner that is relevant to clinical outcomes.[136] PET spatial resolution is generally low relative to the thickness of the cortex, making confident assignment of TSPO PET signal difficult. However, the use of high-resolution PET systems, including PET high resolution research tomographic (PET/HRRT) imaging as well as the integrated PET-MR 'Brain-PET' scanner, offers a substantial increase in spatial resolution compared to other whole-body PET scanners. Additionally, postprocessing strategies based on surface-based analysis can be employed to reduce partial volume effects in the cortex. Compared to volumetric approaches, these methods have been shown to improve the reliability of PET for detecting cortical signal changes.[136]

Statements and recommendations

(1) Initial evidence suggests the presence of PRLs in the cortical grey matter of patients with multiple sclerosis.
(2) Although candidate methods with preliminary data exist (e.g. unwrapped/filtered phase, TSPO-PET), there are currently no well validated techniques for identification of chronic inflammation in grey matter lesions.

Knowledge gap

Additional studies focused on the cortex or other grey matter structures are needed to: (i) assess the role of grey matter PRLs in patients with multiple sclerosis; and (ii) standardize ways to define and monitor them.

Slowly expanding lesions and their association with white matter chronic active lesions

Discussion

As recently defined in the MRI literature,[137] SELs represent areas of pre-existing T_2 lesions that show slow, constant, gradual and radial expansion over a longitudinal T_1-weighted and T_2-weighted MRIs, where expansion over time is assessed using non-linear registration. This registration method is fundamental because the measure of expansion, derived from the computed non-linear deformation (e.g. the Jacobian determinant, which is the determinant of the derivative of the non-linear deformation field), is interpreted as a quantification of local volume expansion. At least three time points, ideally acquired over a period of 1 to 2 years, are required to evaluate the constancy of the observed expansion and ensure that it is gradual over time and not due to an abrupt change secondary to acute re-inflammation of an existing lesion or appearance of a new acute lesion adjacent to a chronic one.

Like PRLs, SELs represent more aggressive lesions and are associated with a more severe clinical and radiological course. Cross-sectional measurements of tissue integrity show that SELs correspond to regions within the T_2-weighted lesions with greater tissue damage,[137–139] while longitudinal studies confirm ongoing tissue degeneration over time, as compared to the rest of the T_2-weighted lesion volume.[138,139] Although GBCA re-enhancement may be responsible for nearly 15% of enhancing lesions,[140,141] this is rarely observed in SELs.[137] Clinical-MRI correlative studies point toward associations between SELs and worse outcomes.[142–145] SELs are detected in both relapsing and progressive multiple sclerosis and are seen more frequently in people with active disease (e.g. new lesion formation over time).[137,142] Patients with multiple slcerosis demonstrating at least one SEL have more advanced physical disability.[138,145] Larger SEL volumes and higher proportions of T_2-lesions identified as SELs predict Expanded Disability Status Scale (EDSS) worsening 7 and 9 years later, respectively.[138,143] SELs exhibit

longitudinal reduction of signal intensity on T_1-weighted sequences and magnetization transfer ratio values.[139] Changes in T_1-weighted lesion volume and T_1-weighted signal intensity within SELs over 120 weeks predict subsequent disability progression.[144]

Some disease-modifying therapies may have a modest effect on the number and volume of SELs,[142,144,146,147] although it remains unclear if this is a direct effect on SELs or an indirect effect due to suppression of acute inflammation, given the strong association between GBCA-enhancing lesions and new T_2-weighted lesions and SELs.

SELs and PRLs have moderate-to-high subject-level correlations but only modest spatial co-localization, indicating that the two lesion types may only partially overlap and identify different biological processes.[128,148] Heterogeneity in PRL volume changes, e.g. enlargement versus stability[45,50,98] or resolution,[23] can at least partially explain why only ~40% of PRLs (or fewer) are also detected as SELs.[148] Data so far suggest that fewer than 20% of SELs[148] and as low as 7%,[128] co-localize with PRLs, and the subset that co-localizes shows increased microstructural tissue damage and ongoing tissue degeneration over time.[148] Some SELs that do not co-localize with PRLs may represent CAL without detectable iron at the lesion edge.[15] It remains possible that others represent additional sources of lesion expansion, such as neurodegeneration of the lesion core and surrounding tissue. Although the gradual expansion and lack of measured GBCA-enhancement at the assessed time points make it unlikely that re-enhancing lesions are determinants of SELs, chronic inflammation sustained by chronic leakage of the blood–brain barrier may also be a responsible factor. Slow degeneration of previously damaged myelin and/or axons, and tissue damage secondary to vascular co-morbidities, are also additional potential culprits.

Statements and recommendations

(1) SELs represent concentrically and gradually expanding areas of focal tissue damage with high tissue destruction not associated with ongoing GBCA-enhancement.
(2) SELs are associated with disability progression.
(3) SELs can be detected using conventional T_1-weighted and T_2-weighted sequences and do not require the acquisition of susceptibility-sensitive MRI. They do, however, require a minimum of three scans, ideally over a period of 1 to 2 years.
(4) SELs and PRLs show only modest co-localization and should not be equated. SELs are identified longitudinally based on observed lesion expansion over time, while PRLs are detected cross-sectionally based on the susceptibility changes induced by iron-laden microglia.
(5) Current methods for SEL detection on MRI have been based on non-linear registration and Jacobian analysis. Optimization of current methods for quantifying lesion expansion and incorporating of intensity-based features of chronic lesion evolution may provide improved markers of chronic lesion activity using conventional MRI.

Knowledge gap

Further studies are required to: (i) better understand the biological underpinnings of SELs and specifically the pathological correlation of SELs and CAL; (ii) assess the optimal follow-up duration for accurate SEL identification as well as the effect of heterogeneity in data acquisition; and (iii) test the efficacy of different methods in detecting SELs.

TSPO-PET to image white matter chronic active lesions

Discussion

^{11}C-PK11195-PET (PK-PET) is a first-generation ligand binding the 18 kDa TSPO, which is expressed on the outer mitochondria membrane of activated myeloid cells[149,150] and has been used to demonstrate increased innate immune activity throughout the brain in patients with multiple sclerosis.[151–155] As a subset of CAL lack a rim of iron-laden myeloid cells[15]; susceptibility-sensitive MRI may underestimate the burden of these lesions, which PET may capture. PK-PET has provided *in vivo* validation that PRLs exhibit higher inflammation compared to rimless lesions.[41] Although PET provides higher molecular specificity than MRI, limitations of spatial resolution impact specific localization of molecular binding within smaller regions of interest.[156,157] As such, some studies have combined chronic lesions as a single target region to explore the impact of therapy.[153,158–160]

Although evaluation of longitudinal inflammatory change within individual chronic lesions would be most informative for treatment studies, technical variability needs to be considered.[161] More recently, a voxel-based parametric approach with TSPO PET has been suggested to identify chronic lesions with increased myeloid cell activity[162–164] and may provide an opportunity to identify CAL beyond those identified with GRE MRI. Interestingly, the majority of TSPO+ lesions demonstrate a homogenous pattern of activation, whereas only a minority have binding localized to the rim. These observations raise the possibility that TSPO PET may identify different phenotypes of chronic lesions, but the interpretation needs further histopathological validation. Importantly, TSPO PET studies should be interpreted with caution as TSPO can also be expressed by astrocytes.[165] Additionally, recent studies suggest that TSPO binds differentially to different subtypes of microglia,[166,167] though within CAL, the predominant binding was to reactive microglia. Notwithstanding these considerations, TSPO PET studies that identify rim-active and uniformly active chronic lesions[164,168] have established an association with subsequent disability, emphasizing the role of these lesion patterns in the progression of the disease.

Newer generation TSPO ligands have improved specificity and brain penetration compared to PK-PET[169–174] and may advance the potential for PET to identify and compare inflammatory activity across individual chronic lesions. Although there are multiple challenges, including variability in quantification approaches to avoid arterial sampling,[175,176] the need for an on-site cyclotron for ^{11}C ligands, repeated radiation exposure for treatment monitoring, and genetic differences in binding affinity with some TSPO ligands, the expanded use of TSPO PET to define CAL may soon be feasible with the development of fluorinated (^{18}F) radiotracers[134,170] and multicentre collaborations.[177]

Statements and recommendations

(1) TSPO is currently the only target for widely available PET tracers for activated microglia/macrophages and astrocytes.
(2) TSPO PET can provide lesion-level *in vivo* support for innate immune system activity in PRLs.
(3) TSPO PET allows for improved molecular specificity to detect a broader population of CALs, however the feasibility of TSPO PET for clinical practice remains limited.
(4) Histopathologic validation of TSPO positive lesions that do not correspond to PRLs is lacking.

Knowledge gap

Studies are needed to: (i) further validate the specific threshold of TSPO ligand uptake within an individual multiple sclerosis lesion to accurately define CAL; and (ii) optimize PET spatial resolution to better meet the needs of CAL visibility.

Imaging white matter chronic active lesions in clinical trials

Discussion

Imaging outcome markers thought to reflect CAL, including PRLs, SELs and TSPO PET, are increasingly being integrated into the design of phase 2 and 3 clinical trials,[178] or in post-marketing studies[129,179] as reflected in listings in the clinicaltrials.gov database.[180–184] Additional multicentre trials are known to be implementing such measures as exploratory outcomes without explicit listing on clinicaltrials.gov.[178] This development reflects a widespread recognition that CAL are an important driver of progressive disability accumulation independent of relapse activity. It also emphasizes the current lack of data regarding the efficacy of existing disease-modifying therapies in preventing or abrogating the biology of progression and its contribution to clinical outcomes. Observations that PRLs are present on scans of patients with multiple sclerosis taking many of the approved therapies, including highly effective medications such as ocrelizumab and natalizumab,[45,129] suggest that distinct treatment strategies, such as those that impact myeloid cells rather than lymphocytes alone, might be required to resolve inflammation within PRLs.

The published use of PRLs as a primary outcome measure to assess either prevention or resolution of CAL is currently limited to single-centre studies,[185–187] and the same is true for TSPO PET[182,188]; no data from prospective clinical trials have been published. In addition, retrospective analyses of clinical trial and natural history datasets have been performed to determine whether existing disease-modifying treatments might modulate these imaging measures, with some early success.[139,144,146,153,158,160,179] Optimal trial designs for studies using pre-existing PRL resolution as an outcome measure are not yet known, although early data reporting that the time span for spontaneous resolution of PRL is inn the order of 5–10 years after they form.[23,50,97] This factor implies that the opportunity for accelerating such resolution within the timeframe of clinical trials may be large. Preliminary calculations suggest that in a 1-year trial, 16 patients per arm, with a total of 112 PRLs, would be sufficient to detect a 10% treatment effect (number of PRLs that fade or disappear) with 80% power.[23] Screening participants based on the presence/absence of PRLs at baseline may increase the statistical power of the studies.

Statements and recommendations

(1) Dynamic biomarkers of CAL (PRLs, SELs and possibly lesions on TSPO-PET) are promising outcome measures in clinical trials assessing the effect of medications on chronic parenchymal inflammatory injury and non-relapsing progressive biology.

Knowledge gap

Investigations are need to: (i) establish optimal trial designs for interventions seeking to resolve CAL; and (ii) determine how best to assess CAL resolution and modulation, e.g. number and proportion of PRL/SEL/TSPO-positive lesions on PET, lesion size, quantitative or comparative features of the lesion core or rim, and association with clinical status.

Conclusions

Over the past decade, the discoveries of PRLs and SELs on MRI, and TSPO-positive lesions on PET, have opened a window into visualization of innate immune activity *in vivo*. PRLs, SELs and TSPO-positive lesions are emerging as potential dynamic biomarkers of the clinical consequences of non-relapsing progressive biology and could lead to a breakthrough in the monitoring of ongoing tissue injury in multiple sclerosis. While partially overlapping, these biomarkers do not have equivalent sensitivity and specificity to histopathologic CAL and thus should not be considered interchangeable. Currently, PRL is the biomarker with the most robust histopathological substantiation. Here, we propose a standardized approach to identify PRLs in the context of non-GBCA-enhancing, sharply demarcated T_2-lesions as well as larger confluent lesions.

Our initial standardization is based upon research experience of the authors as well as current literature. We realize that more research is needed to test our proposed definitions. For example, our proposed definition may not apply to all MRI acquisition methods; it also needs to be compared to other less or more stringent criteria and should be ideally tested against histology.

Further research is also needed to compare the efficacy and feasibility of each susceptibility-sensitive MRI method for detecting PRLs as well as to develop standards and tools for PRL quantification. Last, while PRLs have been detected on images with submillimetre in-plane and <3-mm through-plane resolution, work is needed to understand the efficiency of low-resolution sequences in detecting all PRLs.

However, standardizing definitions is at this stage a stepping stone to facilitate inter-study comparisons and move the field forward.

We also provide an appraisal of current knowledge on the role of PRLs, SELs and TSPO lesions as disability indicators and outcome prognosticators, and we identify knowledge gaps to set the stage for future research. We obtained consensus that PRLs represent a pathophysiological biomarker of multiple sclerosis that warrants additional clinical attention. Whether these lesions are causative of accelerated disability accumulation of course or rather an epiphenomenon requires additional investigation.

Such research should, among other things, further assess the biological and clinical role of PRLs and foster the development of measurement tools to allow monitoring of PRLs in both proof-of-concept clinical trials and day-to-day clinical practice.

Acknowledgements

We gratefully acknowledge the support of Mrs Emily Viles-Monari (NAIMS Cooperative) in planning the NAIMS workshop. We thank all the NAIMS workshop participants for the fruitful discussion the day of the workshop. We extend a note of special gratitude to Dr Amit Bar-Or (Department of Neurology, Perelman School of Medicine, University of Pennsylvania, Philadelphia, PA, USA), and Dr Robert Zivadinov (Buffalo Neuroimaging Analysis Center, Department of Neurology, Jacobs School of Medicine and Biomedical Sciences and Center for Biomedical Imaging at Clinical Translational Science Institute, University at Buffalo, State University of New York, Buffalo, NY, USA), for reading the manuscript and providing insightful comments and to Mrs Taegan Vinersky for editorial aid.

This manuscript is dedicated to the sweet memory of Mr Oscar Castro.

Funding

M.A. receives research support from the Conrad N. Hilton Foundation (17313), the Cariplo Foundation (2019–1677), the Fondazione

Regionale per la Ricerca Biomedica (1750327), the National Multiple Sclerosis Society (RFA-2203-39325) and the International Progressive MS Alliance (PA-2107-38081). C.J.A. receives research support from the National Multiple Sclerosis Society (RG-1802-30140, JF-2008-36971, and AWD-00005884) and the National Institutes of Health (U01NS116776-01). F.B. receives research support from the National Multiple Sclerosis Society (RG-1901-33190), the National Institutes of Health (NIH) (R21 NS116434-01A1), the Veterans Health Administration (I01CX002160-01A1) and the Voros Innovation Impact Funds. P.A.C. receives research support from the National Institutes of Health (R01NS082347), Genentech and previously Principia Biopharma. S.A.G. research programme is funded by Myelin Repair Foundation, Genentech and the National Institute of Neurological Disorders and Stroke of the National Institutes of Health (R01 NS104283, R01 105144). D.M.H. receives funding from the National Institute of Neurological Disorders and Stroke of the National Institutes of Health (1R01NS122980-01 and 1R01NS104403-01), the Department of Defense (MS210103), The National MS Society (RG-2110-38460), and Roche-Genentech. C.C.H. receives research support from the NIH-NINDS (K23NS126718), the National Center for Advancing Translational Sciences, NIH (KL2TR001454) and National Multiple Sclerosis Society (PP-1809-32498). R.G.H. receives research support from Roche, Genentech, Atara Biotherapeutics, National Multiple Sclerosis Society RG-1707-28775, Department of Defense W81XWH-14-1-0493. C.L. receives research support from the Natural Sciences and Engineering Research Council of Canada (NSERC), the Craig H. Neilsen Foundation and the International Collaboration on Repair Discoveries (ICORD). C.M. receives research support from NIH (1R21NS1226737-01, 1R21NS123419-01 and R01DA047088-01), the National MS Society (RG-1802-30468) and Genentech. J.O. receives research support from the Multiple Sclerosis Society of Canada, the National MS Society, Brain Canada, and National Institutes of Health (1U01NS116776-01). D.O. receives research support from the NIH (U01 NS116776-01, R35 NS097303, R56 NR019306-01A1), the Patient Centered Outcomes Research Institute (MS-1610-37047), the Department of Defense (W81XWH2110787), and the National Multiple Sclerosis Society (RG-1902-33619). D.P. receives research support from the National Institutes of Health (R01 NS102267, R01 NS112907, R01 NS118886, R21 NS129197), the Department of Defense (W81XWH2010580) and the National Multiple Sclerosis Society (SI-2004-36589). D.S.R. is supported by the Intramural Research Program of National Institute of Neurological Disorders and Stroke of the National Institutes of Health (Z01 NS003119). W.D.R. received research support from the Myelin Repair Foundation, Conrad N. Hilton Foundation, NIH/NINDS (R01 NS40801, R01-EB007258). P.S. receives research support from the National MS Society (RG-2110-38526), NIH (U01 NS116776-01), and the Erwin Rautenberg Foundation. R.T.S. receives research support from the National Institutes of Health (R01 NS 112274, R01 MH 123550, R01 MH 112847, R01 NS060910, and U01 NS116776). N.L.S. receives support from the National Institutes of Health (U01 NS116776-01), Patient Centered Outcomes Research Institute (MS-1610-37115). B.T. receives research support from the National Institutes of Health (R35NS097303).

Competing interests

M.A. received consultancy income from Sanofi, Biogen, Abata Therapeutics and Glaxo Smith Klein. C.J.A. has received consulting income from Horizon Therapeutics, Genentech, Sanofi Genzyme, Alexion, EMD Serono, and Novartis; compensation for scientific reviewing from the Department of Defense; and honoraria related to creating educational content for Projects in Knowledge, Catamount Education, and Spire Learning. F.B. received consultancy income from Sanofi-Genzyme; Biogen, Janssen Pharmaceuticals and EMD Serono and receives compensation for scientific reviewing from the National Institutes of Health. P.A.C. received consulting honoraria for serving on SABs for Nervgen, Idorsia, Biogen, Vaccitech, and Lilly. C.E. is an employee of NeuroRx Research and received speaking honoraria from EMD Serono; S.A.G. has received consultancy income from Genentech. D.M.H. received consulting income from EMD Serono and Horizon Therapeutics, writing fees from the American College of Physicians, and royalties from Up To Date, Inc. C.C.H. receives consultancy income from VIVIO Health. J.O. has received research funding from Biogen-Idec, Roche, and EMD-Serono and has received consultancy income from Biogen-Idec, Roche, Sanofi-Genzyme, Novartis, and BMS. D.O. receives research funding from BMS, Genentech, Genzyme, and Novartis; and consulting fees from Biogen Idec, BMS, Genentech/Roche, Genzyme, Janssen, Novartis, Merck, and Pipeline Thrapeutics. D.S.R. has received research funding from Abata Therapeutics and Sanofi-Genzyme. W.D.R. received research funding from Revalesio, Inc, and is a consultant with Ultragenyx. R.T.S. received consulting income from Octave Bioscience and has received compensation for scientific reviewing from the American Medical Association, the Department of Defense, the Emerson Collective, and the National Institutes of Health. B.T. receives speaking fees from Sanofi-Genzyme, advisory board fees from Disarm Therapeutics, Therini Bio. Inc. and Sanofi-Genzyme.

Supplementary material

Supplementary material is available at *Brain* online.

References

1. Katz D, Taubenberger JK, Cannella B, McFarlin DE, Raine CS, McFarland HF. Correlation between magnetic resonance imaging findings and lesion development in chronic, active multiple sclerosis. *Ann Neurol*. 1993;34:661-669.
2. McFarland HF. The lesion in multiple sclerosis: Clinical, pathological, and magnetic resonance imaging considerations. *J Neurol Neurosurg Psychiatry*. 1998;64(S1):S26-S30.
3. Harris JO, Frank JA, Patronas N, McFarlin DE, McFarland HF. Serial gadolinium-enhanced magnetic resonance imaging scans in patients with early, relapsing-remitting multiple sclerosis: Implications for clinical trials and natural history. *Ann Neurol*. 1991;29:548-555.
4. Stone LA, Smith ME, Albert PS, et al. Blood-brain barrier disruption on contrast-enhanced MRI in patients with mild relapsing-remitting multiple sclerosis: Relationship to course, gender, and age. *Neurology*. 1995;45:1122-1126.
5. Smith ME, Stone LA, Albert PS, et al. Clinical worsening in multiple sclerosis is associated with increased frequency and area of gadopentetate dimeglumine-enhancing magnetic resonance imaging lesions. *Ann Neurol*. 1993;33:480-489.
6. Prineas JW, Kwon EE, Cho ES, et al. Immunopathology of secondary-progressive multiple sclerosis. *Ann Neurol*. 2001;50:646-657.
7. Prineas JW, Connell F. Remyelination in multiple sclerosis. *Ann Neurol*. 1979;5:22-31.
8. Pitt D, Boster A, Pei W, et al. Imaging cortical lesions in multiple sclerosis with ultra-high-field magnetic resonance imaging. *Arch Neurol*. 2010;67:812-818.

9. Gilmore CP, Geurts JJ, Evangelou N, et al. Spinal cord grey matter lesions in multiple sclerosis detected by post-mortem high field MR imaging. *Mult Scler*. 2009;15:180-188.
10. Waldman AD, Catania C, Pisa M, Jenkinson M, Lenardo MJ, DeLuca GC. The prevalence and topography of spinal cord demyelination in multiple sclerosis: a retrospective study. *Acta Neuropathol*. 2024;147:51.
11. Kuhlmann T, Ludwin S, Prat A, Antel J, Brück W, Lassmann H. An updated histological classification system for multiple sclerosis lesions. *Acta Neuropathol*. 2017;133:13-24.
12. Lee NJ, Ha SK, Sati P, et al. Spatiotemporal distribution of fibrinogen in marmoset and human inflammatory demyelination. *Brain*. 2018;141:1637-1649.
13. Frischer JM, Weigand SD, Guo Y, et al. Clinical and pathological insights into the dynamic nature of the white matter multiple sclerosis plaque. *Ann Neurol*. 2015;78:710-721.
14. Luchetti S, Fransen NL, van Eden CG, Ramaglia V, Mason M, Huitinga I. Progressive multiple sclerosis patients show substantial lesion activity that correlates with clinical disease severity and sex: A retrospective autopsy cohort analysis. *Acta Neuropathol*. 2018;135:511-528.
15. Popescu BF, Frischer JM, Webb SM, et al. Pathogenic implications of distinct patterns of iron and zinc in chronic MS lesions. *Acta Neuropathol*. 2017;134:45-64.
16. Pitt D, Lo CH, Gauthier SA, et al. Toward precision phenotyping of multiple sclerosis. *Neurol Neuroimmunol Neuroinflamm*. 2022;9:e200025.
17. Kuhlmann T, Moccia M, Coetzee T, et al. Multiple sclerosis progression: Time for a new mechanism-driven framework. *Lancet Neurol*. 2023;22:78-88.
18. Oh J, Bakshi R, Calabresi PA, et al. The NAIMS cooperative pilot project: Design, implementation, and future directions. *Mult Scler*. 2017;24:1770-1772.
19. North American Imaging in MS Cooperative Workshop, February 23, 2022. https://www.naimscooperative.org/2022-naims-workshop
20. Masuda T, Sankowski R, Staszewski O, et al. Spatial and temporal heterogeneity of mouse and human microglia at single-cell resolution. *Nature*. 2019;566:388-392.
21. Schirmer L, Velmeshev D, Holmqvist S, et al. Neuronal vulnerability and multilineage diversity in multiple sclerosis. *Nature*. 2019;573:75-82.
22. Jäkel S, Agirre E, Mendanha Falcão A, et al. Altered human oligodendrocyte heterogeneity in multiple sclerosis. *Nature*. 2019;566:543-547.
23. Absinta M, Maric D, Gharagozloo M, et al. A lymphocyte–microglia–astrocyte axis in chronic active multiple sclerosis. *Nature*. 2021;597:709-714.
24. Liddelow SA, Guttenplan KA, Clarke LE, et al. Neurotoxic reactive astrocytes are induced by activated microglia. *Nature*. 2017;541:481-487.
25. Wheeler MA, Clark IC, Tjon EC, et al. MAFG-driven astrocytes promote CNS inflammation. *Nature*. 2020;578:593-599.
26. Rissanen E, Virta JR, Paavilainen T, et al. Adenosine A2A receptors in secondary progressive multiple sclerosis: A [11C] TMSX brain PET study. *J Cereb Blood Flow Metab*. 2013;33:1394-1401.
27. Sanmarco LM, Wheeler MA, Gutiérrez-Vázquez C, et al. Gut-licensed IFNγ+ NK cells drive LAMP1 + TRAIL+ anti-inflammatory astrocytes. *Nature*. 2021;590:473-479.
28. Olah M, Menon V, Habib N, et al. Single cell RNA sequencing of human microglia uncovers a subset associated with Alzheimer's disease. *Nat Commun*. 2020;11:6129.
29. Krasemann S, Madore C, Cialic R, et al. The TREM2-APOE pathway drives the transcriptional phenotype of dysfunctional microglia in neurodegenerative diseases. *Immunity*. 2017;47:566-581.e9.
30. Peterson JW, Bö L, Mörk S, Chang A, Trapp BD. Transected neurites, apoptotic neurons, and reduced inflammation in cortical multiple sclerosis lesions. *Ann Neurol*. 2001;50:389-400.
31. Bevan RJ, Evans R, Griffiths L, et al. Meningeal inflammation and cortical demyelination in acute multiple sclerosis. *Ann Neurol*. 2018;84:829-842.
32. Lucchinetti CF, Popescu BF, Bunyan RF, et al. Inflammatory cortical demyelination in early multiple sclerosis. *N Engl J Med*. 2011;365:2188-2197.
33. Magliozzi R, Howell OW, Reeves C, et al. A gradient of neuronal loss and meningeal inflammation in multiple sclerosis. *Ann Neurol*. 2010;68:477-493.
34. Ciccarelli O, Giugni E, Paolillo A, et al. Magnetic resonance outcome of new enhancing lesions in patients with relapsing-remitting multiple sclerosis. *Eur J Neurol*. 1999;6:455-459.
35. Bagnato F, Jeffries N, Richert ND, et al. Evolution of T1 black holes in patients with multiple sclerosis imaged monthly for 4 years. *Brain*. 2003;126:1782-1789.
36. Cotton F, Weiner HL, Jolesz FA, Guttmann CR. MRI contrast uptake in new lesions in relapsing-remitting MS followed at weekly intervals. *Neurology*. 2003;60(4):640-646.
37. Bagnato F, Hametner S, Yao B, et al. Tracking iron in multiple sclerosis: A combined imaging and histopathological study at 7 Tesla. *Brain*. 2011;134:3602-3615.
38. Yao B, Bagnato F, Matsuura E, et al. Chronic multiple sclerosis lesions: Characterization with high-field-strength MR imaging. *Radiology*. 2012;262:206-215.
39. Walsh AJ, Lebel RM, Eissa A, et al. Multiple sclerosis: Validation of MR imaging for quantification and detection of iron. *Radiology*. 2013;267:531-542.
40. Dimov AV, Gillen KM, Nguyen TD, et al. Magnetic susceptibility source separation solely from gradient echo data: Histological validation. *Tomography*. 2022;8:1544-1551.
41. Kaunzner UW, Kang Y, Zhang S, et al. Quantitative susceptibility mapping identifies inflammation in a subset of chronic multiple sclerosis lesions. *Brain*. 2019;142:133-145.
42. Gillen KM, Mubarak M, Park C, et al. QSM is an imaging biomarker for chronic glial activation in multiple sclerosis lesions. *Ann Clin Transl Neurol*. 2021;8:877-886.
43. Rahmanzadeh R, Galbusera R, Lu PJ, et al. A new advanced MRI biomarker for remyelinated lesions in multiple sclerosis. *Ann Neurol*. 2022;92:486-502.
44. Absinta M, Sati P, Schindler M, et al. Persistent 7-Tesla phase rim predicts poor outcome in new multiple sclerosis patient lesions. *J Clin Invest*. 2016;126:2597-2609.
45. Absinta M, Sati P, Masuzzo F, et al. Association of chronic active multiple sclerosis lesions with disability in vivo. *JAMA Neurol*. 2019;76:1474-1483.
46. Maggi P, Kuhle J, Schädelin S, et al. Chronic white matter inflammation and serum neurofilament levels in multiple sclerosis. *Neurology*. 2021;97:e543-e553.
47. Kolb H, Absinta M, Beck ES, et al. 7T MRI differentiates remyelinated from demyelinated multiple sclerosis lesions. *Ann Neurol*. 2021;90:612-626.
48. Absinta M, Sati P, Gaitán MI, et al. Seven-tesla phase imaging of acute multiple sclerosis lesions: A new window into the inflammatory process. *Ann Neurol*. 2013;74:669-678.
49. Dal-Bianco A, Grabner G, Kronnerwetter C, et al. Slow expansion of multiple sclerosis iron rim lesions: Pathology and 7 T magnetic resonance imaging. *Acta Neuropathol*. 2017;133:25-42.
50. Dal-Bianco A, Grabner G, Kronnerwetter C, et al. Long-term evolution of multiple sclerosis iron rim lesions in 7 T MRI. *Brain*. 2021;144:833-847.

51. Yao B, Ikonomidou VN, Cantor FK, Ohayon JM, Duyn J, Bagnato F. Heterogeneity of multiple sclerosis white matter lesions detected with T2*-weighted imaging at 7.0 tesla. *J Neuroimaging*. 2015;25:799-806.
52. Chawla S, Kister I, Wuerfel J, et al. Iron and non-iron-related characteristics of multiple sclerosis and neuromyelitis optica lesions at 7T MRI. *Am J Neuroradiol*. 2016;37:1223-1230.
53. Harrison DM, Li X, Liu H, et al. Lesion heterogeneity on high-field susceptibility MRI is associated with multiple sclerosis severity. *Am J Neuroradiol*. 2016;37:1447-1453.
54. Chen W, Gauthier SA, Gupta A, et al. Quantitative susceptibility mapping of multiple sclerosis lesions at various ages. *Radiology*. 2014;271:183-192.
55. Pooley RA. Fundamental physics of MR imaging. *RadioGraphics*. 2005;25:1087-1099.
56. Wisnieff C, Ramanan S, Olesik J, Gauthier S, Wang Y, Pitt D. Quantitative susceptibility mapping (QSM) of white matter multiple sclerosis lesions: Interpreting positive susceptibility and the presence of iron. *Magn Reson Med*. 2014;74:564-570.
57. Siemonsen S, Young KL, Bester M, et al. Chronic T2 lesions in multiple sclerosis are heterogeneous regarding phase MR imaging. *Clin Neuroradiol*. 2016;26:457-464.
58. Jang J, Nam Y, Choi Y, et al. Paramagnetic rims in multiple sclerosis and neuromyelitis optica spectrum disorder: A quantitative susceptibility mapping study with 3-T MRI. *J Clin Neurol*. 2020;16:562-572.
59. Clarke MA, Pareto D, Pessini-Ferreira L, et al. Value of 3T susceptibility-weighted imaging in the diagnosis of multiple sclerosis. *Am J Neuroradiol*. 2020;41:1001-1008.
60. Caruana G, Pessini LM, Cannella R, et al. Texture analysis in susceptibility-weighted imaging may be useful to differentiate acute from chronic multiple sclerosis lesions. *Eur Radiol*. 2020;30:6348-6356.
61. Weber CE, Krämer J, Wittayer M, et al. Association of iron rim lesions with brain and cervical cord volume in relapsing multiple sclerosis. *Eur Radiol*. 2022;32:2012-2022.
62. Sati P, Thomasson D, Li N, et al. Rapid, high-resolution, whole-brain, susceptibility-based MRI of multiple sclerosis. *Mult Scler*. 2014;20:1464-1470.
63. Absinta M, Sati P, Fechner A, Schindler MK, Nair G, Reich DS. Identification of chronic active multiple sclerosis lesions on 3T MRI. *Am J Neuroradiol*. 2018;39:1233-1238.
64. Maggi P, Sati P, Nair G, et al. Paramagnetic rim lesions are specific to multiple sclerosis: An international multicenter 3T MRI study. *Ann Neurol*. 2020;88:1034-1042.
65. Ng Kee Kwong KC, Mollison D, Meijboom R, et al. Rim lesions are demonstrated in early relapsing-remitting multiple sclerosis using 3T-based susceptibility-weighted imaging in a multi-institutional setting. *Neuroradiology*. 2022;64:109-117.
66. Pinto C, Cambron M, Dobai A, Vanheule E, Casselman JW. Smoldering lesions in MS: If you like it then you should put a rim on it. *Neuroradiology*. 2022;64:703-714.
67. Haller S, Haacke EM, Thurnher MM, Barkhof F. Susceptibility-weighted imaging: Technical essentials and clinical neurologic applications. *Radiology*. 2021;299:3-26.
68. Schofield MA, Zhu Y. Fast phase unwrapping algorithm for interferometric applications. *Opt Lett*. 2003;28:1194.
69. He W, Xia L, Liu F. Sparse-representation-based direct minimum L (p) -norm algorithm for MRI phase unwrapping. *Comput Math Methods Med*. 2014;2014:134058.
70. Li N, Wang WT, Sati P, Pham DL, Butman JA. Quantitative assessment of susceptibility weighted imaging processing methods. *J Magn Reson Imaging*. 2014;40:1463-1473.
71. Li W, Avram AV, Wu B, Xiao X, Liu C. Integrated Laplacian-based phase unwrapping and background phase removal for quantitative susceptibility mapping. *NMR Biomed*. 2014;27:219-227.
72. Schweser F, Deistung A, Lehr BW, Reichenbach JR. Quantitative imaging of intrinsic magnetic tissue properties using MRI signal phase: An approach to in vivo brain iron metabolism? *Neuroimage*. 2011;54:2789-2807.
73. Sun H, Wilman AH. Background field removal using spherical mean value filtering and Tikhonov regularization. *Magn Reson Med*. 2014;71:1151-1157.
74. Eskreis-Winkler S, Deh K, Gupta A, et al. Multiple sclerosis lesion geometry in quantitative susceptibility mapping (QSM) and phase imaging. *J Magn Reson Imaging*. 2015;42:224-229.
75. Cronin MJ, Wharton S, Al-Radaideh A, et al. A comparison of phase imaging and quantitative susceptibility mapping in the imaging of multiple sclerosis lesions at ultrahigh field. *MAGMA*. 2016;29:543-557.
76. Liu C, Li W, Tong KA, Yeom KW, Kuzminski S. Susceptibility-weighted imaging and quantitative susceptibility mapping in the brain. *J Magn Reson Imaging*. 2015;42:23-41.
77. Wharton S, Schfer A, Bowtell R. Susceptibility mapping in the human brain using threshold-based k-space division. *Magn Reson Med*. 2010;63:1292-1304.
78. Liu J, Liu T, de Rochefort L, et al. Morphology enabled dipole inversion for quantitative susceptibility mapping using structural consistency between the magnitude image and the susceptibility map. *Neuroimage*. 2012;59:2560-2568.
79. Schweser F, Sommer K, Deistung A, Reichenbach JR. Quantitative susceptibility mapping for investigating subtle susceptibility variations in the human brain. *Neuroimage*. 2012;62:2083-2100.
80. Wei H, Dibb R, Zhou Y, et al. Streaking artifact reduction for quantitative susceptibility mapping of sources with large dynamic range. *NMR Biomed*. 2015;28:1294-1303.
81. Langkammer C, Bredies K, Poser BA, et al. Fast quantitative susceptibility mapping using 3D EPI and total generalized variation. *Neuroimage*. 2015;111:622-630.
82. Bao L, Li X, Cai C, Chen Z, van Zijl PCM. Quantitative susceptibility mapping using structural feature based collaborative reconstruction (SFCR) in the human brain. *IEEE Trans Med Imaging*. 2016;35:2040-2050.
83. Liu Z, Spincemaille P, Yao Y, Zhang Y, Wang Y. MEDI+0: Morphology enabled dipole inversion with automatic uniform cerebrospinal fluid zero reference for quantitative susceptibility mapping. *Magn Reson Med*. 2017;79:2795-2803.
84. Sati P, Cross AH, Luo J, Hildebolt CF, Yablonskiy DA. In vivo quantitative evaluation of brain tissue damage in multiple sclerosis using gradient echo plural contrast imaging technique. *Neuroimage*. 2010;51:1089-1097.
85. Luo J, Jagadeesan BD, Cross AH, Yablonskiy DA. Gradient echo plural contrast imaging-signal model and derived contrasts: T2*, T1, phase, SWI, T1f, FST2*and T2*-SWI. *Neuroimage*. 2012;60:1073-1082.
86. Hemond CC, Reich DS, Dundamadappa SK. Paramagnetic rim lesions in multiple sclerosis: Comparison of visualization at 1.5-T and 3-T MRI. *Am J Roentgenol*. 2022;219:120-131.
87. Huang W, Sweeney EM, Kaunzner UW, Wang Y, Gauthier SA, Nguyen TD. Quantitative susceptibility mapping versus phase imaging to identify multiple sclerosis iron rim lesions with demyelination. *J Neuroimaging*. 2022;32:667-675.
88. Barquero G, La Rosa F, Kebiri H, et al. RimNet: A deep 3D multimodal MRI architecture for paramagnetic rim lesion assessment in multiple sclerosis. *Neuroimage Clin*. 2020;28:102412.
89. Lou C, Sati P, Absinta M, et al. Fully automated detection of paramagnetic rims in multiple sclerosis lesions on 3T susceptibility-based MR imaging. *Neuroimage Clin*. 2021;32:102796.

90. La Rosa F, Abdulkadir A, Fartaria MJ, et al. Multiple sclerosis cortical and white matter lesion segmentation at 3T MRI: A deep learning method based on FLAIR and MP2RAGE. *Neuroimage Clin*. 2020;27:102335.
91. Valcarcel AM, Linn KA, Vandekar SN, et al. MIMoSA: An automated method for intermodal segmentation analysis of multiple sclerosis brain lesions. *J Neuroimaging*. 2018;28: 389-398.
92. Valcarcel AM, Linn KA, Khalid F, et al. A dual modeling approach to automatic segmentation of cerebral T2 hyperintensities and T1 black holes in multiple sclerosis. *Neuroimage Clin*. 2018;20:1211-1221.
93. Dworkin JD, Linn KA, Oguz I, et al. An automated statistical technique for counting distinct multiple sclerosis lesions. *Am J Neuroradiol*. 2018;39:626-633.
94. Kolossváry M, Karády J, Szilveszter B, et al. Radiomic features are superior to conventional quantitative computed tomographic metrics to identify coronary plaques with napkin-ring sign. *Circ Cardiovasc Imaging*. 2017;10:e006843.
95. Zhang H, Nguyen TD, Zhang J, et al. QSMRim-Net: Imbalance-aware learning for identification of chronic active multiple sclerosis lesions on quantitative susceptibility maps. *Neuroimage Clin*. 2022;34:102979.
96. Wenzel N, Wittayer M, Weber CE, et al. MRI predictors for the conversion from contrast enhancing to iron rim multiple sclerosis lesions. *J Neurol*. 2022;269:4414-4420.
97. Zhang S, Nguyen TD, Hurtado Rúa SM, et al. Quantitative susceptibility mapping of time-dependent susceptibility changes in multiple sclerosis lesions. *Am J Neuroradiol*. 2019;40:987-993.
98. Weber CE, Wittayer M, Kraemer M, et al. Long-term dynamics of multiple sclerosis iron rim lesions. *Mult Scler Relat Disord*. 2022;57:103340.
99. Clark KA, Manning AR, Chen L, et al. Early magnetic resonance imaging features of new paramagnetic rim lesions in multiple sclerosis. *Ann Neurol*. 2023;94:736-744.
100. Choi S, Lake S, Harrison DM. Evaluation of the blood-brain barrier, demyelination, and neurodegeneration in paramagnetic rim lesions in multiple sclerosis on 7 Tesla MRI. *J Magn Reson Imaging*. 2024;59(3):941-951.
101. Ng Kee Kwong KC, Mollison D, Meijboom R, et al. Rim lesions are demonstrated in early relapsing-remitting multiple sclerosis using 3 T-based susceptibility-weighted imaging in a multi-institutional setting. *Neuroradiology*. 2022;64: 109-117.
102. Treaba CA, Conti A, Klawiter EC, et al. Cortical and phase rim lesions on 7 T MRI as markers of multiple sclerosis disease progression. *Brain Commun*. 2021;3:fcab134.
103. Hemond CC, Baek J, Ionete C, Reich DS. Paramagnetic rim lesions are associated with pathogenic CSF profiles and worse clinical status in multiple sclerosis: A retrospective cross-sectional study. *Mult Scler*. 2022;28:2046-2056.
104. Blindenbacher N, Brunner E, Asseyer S, et al. Evaluation of the "ring sign" and the "core sign" as a magnetic resonance imaging marker of disease activity and progression in clinically isolated syndrome and early multiple sclerosis. *Mult Scler J Exp Transl Clin*. 2020;6:2055217320915480.
105. Krajnc N, Schmidbauer V, Leinkauf J, et al. Paramagnetic rim lesions lead to pronounced diffuse periplaque white matter damage in multiple sclerosis. *Mult Scler*. 2023;29:1406-1417.
106. Yao Y, Nguyen TD, Pandya S, et al. Combining quantitative susceptibility mapping with automatic zero reference (QSM0) and myelin water fraction imaging to quantify IronRelated myelin damage in chronic active MS lesions. *Am J Neuroradiol*. 2018; 39:303-310.
107. Rahmanzadeh R, Lu PJ, Barakovic M, et al. Myelin and axon pathology in multiple sclerosis assessed by myelin water and multi-shell diffusion imaging. *Brain*. 2021;144: 1684-1696.
108. Hagemeier J, Heininen-Brown M, Poloni GU, et al. Iron deposition in multiple sclerosis lesions measured by susceptibility-weighted imaging filtered phase: A case control study. *J Magn Reson Imaging*. 2012;36:73-83.
109. Hosseini Z, Matusinec J, Rudko DA, et al. Morphology-Specific discrimination between MS white matter lesions and benign white matter hyperintensities using ultra-HighField MRI. *Am J Neuroradiol*. 2018;39:1473-1479.
110. Sinnecker T, Schumacher S, Mueller K, et al. MRI phase changes in multiple sclerosis vs neuromyelitis optica lesions at 7T. *Neurol Neuroimmunol Neuroinflamm*. 2016;3:e259.
111. Wuerfel J, Sinnecker T, Ringelstein EB, et al. Lesion morphology at 7 tesla MRI differentiates Susac syndrome from multiple sclerosis. *Mult Scler*. 2012;18:1592-1599.
112. Meaton I, Altokhis A, Allen CM, et al. Paramagnetic rims are a promising diagnostic imaging biomarker in multiple sclerosis. *Mult Scler*. 2022;28:2212-2220.
113. Kilsdonk ID, Wattjes MP, Lopez-Soriano A, et al. Improved differentiation between MS and vascular brain lesions using FLAIR* at 7 Tesla. *Eur Radiol*. 2014;24:841-849.
114. Kim W, Shin HG, Lee H, et al. χ-Separation imaging for diagnosis of multiple sclerosis versus neuromyelitis optica spectrum disorder. *Radiology*. 2023;307:e220941.
115. Suthiphosuwan S, Sati P, Absinta M, et al. Paramagnetic rim sign in radiologically isolated syndrome. *JAMA Neurol*. 2020; 77:653.
116. George IC, Rice DR, Chibnik LB, Mateen FJ. Radiologically isolated syndrome: A singlecenter, retrospective cohort study. *Mult Scler Relat Disord*. 2021;55:103183.
117. Marcille M, Hurtado Rúa S, Tyshkov C, et al. Disease correlates of rim lesions on quantitative susceptibility mapping in multiple sclerosis. *Sci Rep*. 2022;12:4411.
118. Comabella M, Clarke MA, Schaedelin S, et al. CSF chitinase 3-like 1 is associated with iron rims in patients with a first demyelinating event. *Mult Scler*. 2021;28:71-81.
119. Guo Z, Long L, Qiu W, et al. The distributional characteristics of multiple sclerosis lesions on quantitative susceptibility mapping and their correlation with clinical severity. *Front Neurol*. 2021;12:647519.
120. Tozlu C, Jamison K, Nguyen T, et al. Structural disconnectivity from paramagnetic rim lesions is related to disability in multiple sclerosis. *Brain Behav*. 2021;11:e2353.
121. Wittayer M, Weber CE, Platten M, Schirmer L, Gass A, Eisele P. Spatial distribution of multiple sclerosis iron rim lesions and their impact on disability. *Mult Scler Relat Disord*. 2022;64: 103967.
122. Wittayer M, Weber CE, Krämer J, et al. Exploring (peri-) lesional and structural connectivity tissue damage through T1/T2-weighted ratio in iron rim multiple sclerosis lesions. *Magn Reson Imaging*. 2023;95:12-18.
123. Wittayer M, Weber CE, Kittel M, et al. Cerebrospinal fluid-related tissue damage in multiple sclerosis patients with iron rim lesions. *Mult Scler*. 2023;29(4–5):549-558.
124. Dal-Bianco A, Schranzer R, Grabner G, et al. Iron rims in patients with multiple sclerosis as neurodegenerative marker? A 7-tesla magnetic resonance study. *Front Neurol*. 2021;12: 632749.
125. Lewin A, Hamilton S, Witkover A, et al. Free serum haemoglobin is associated with brain atrophy in secondary progressive multiple sclerosis. *Wellcome Open Res*. 2016;1:10.

126. Krajnc N, Bsteh G, Kasprian G, et al. Peripheral hemolysis in relation to iron rim presence and brain volume in multiple sclerosis. *Front Neurol*. 2022;13:928582.
127. Altokhis AI, Hibbert AM, Allen CM, et al. Longitudinal clinical study of patients with iron rim lesions in multiple sclerosis. *Mult Scler*. 2022;28:2202-2211.
128. Calvi A, Clarke MA, Prados F, et al. Relationship between paramagnetic rim lesions and slowly expanding lesions in multiple sclerosis. *Mult Scler*. 2023;29:352-362.
129. Maggi P, Bulcke CV, Pedrini E, et al. B cell depletion therapy does not resolve chronic active multiple sclerosis lesions. *EBioMedicine*. 2023;94:104701.
130. Mainero C, Benner T, Radding A, et al. In vivo imaging of cortical pathology in multiple sclerosis using ultra-high field MRI. *Neurology*. 2009;73:941-948.
131. Castellaro M, Magliozzi R, Palombit A, et al. Heterogeneity of cortical lesion susceptibility mapping in multiple sclerosis. *Am J Neuroradiol*. 2017;38:1087-1095.
132. Shin HG, Lee J, Yun YH, et al. χ-separation: Magnetic susceptibility source separation toward iron and myelin mapping in the brain. *Neuroimage*. 2021;240:118371.
133. Politis M, Giannetti P, Su P, et al. Increased PK11195 PET binding in the cortex of patients with MS correlates with disability. *Neurology*. 2012;79:523-530.
134. Herranz E, Giannì C, Louapre C, et al. Neuroinflammatory component of gray matter pathology in multiple sclerosis. *Ann Neurol*. 2016;80:776-790.
135. Singhal T, O'Connor K, Dubey S, et al. Gray matter microglial activation in relapsing vs progressive MS: A [F-18]PBR06-PET study. *Neurol Neuroimmunol Neuroinflamm*. 2019;6:e587.
136. Herranz E, Louapre C, Treaba CA, et al. Profiles of cortical inflammation in multiple sclerosis by 11C-PBR28 MR-PET and 7 Tesla imaging. *Mult Scler*. 2019;26:1497-1509.
137. Elliott C, Wolinsky JS, Hauser SL, et al. Slowly expanding/evolving lesions as a magnetic resonance imaging marker of chronic active multiple sclerosis lesions. *Mult Scler*. 2019;25:1915-1925.
138. Calvi A, Tur C, Chard D, et al. Slowly expanding lesions relate to persisting black-holes and clinical outcomes in relapse-onset multiple sclerosis. *Neuroimage Clin*. 2022;35:103048.
139. Elliott C, Arnold DL, Chen H, et al. Patterning chronic active demyelination in slowly expanding/evolving white matter MS lesions. *Am J Neuroradiol*. 2020;41:1584-1591.
140. Gupta S, Solomon JM, Tasciyan TA, et al. Interferon-beta-1b effects on re-enhancing lesions in patients with multiple sclerosis. *Mult Scler*. 2005;11:658-668.
141. Davis M, Auh S, Riva M, et al. Ring and nodular multiple sclerosis lesions. *Neurology*. 2010;74:851-856.
142. Beynon V, George IC, Elliott C, et al. Chronic lesion activity and disability progression in secondary progressive multiple sclerosis. *BMJ Neurol Open*. 2022;4:e000240.
143. Preziosa P, Pagani E, Meani A, et al. Slowly expanding lesions predict 9-year multiple sclerosis disease progression. *Neurol Neuroimmunol Neuroinflamm*. 2022;9:e1139.
144. Elliott C, Belachew S, Wolinsky JS, et al. Chronic white matter lesion activity predicts clinical progression in primary progressive multiple sclerosis. *Brain*. 2019;142:2787-2799.
145. Calvi A, Carrasco FP, Tur C, et al. Association of slowly expanding lesions on MRI with disability in people with secondary progressive multiple sclerosis. *Neurology*. 2022;98:e1783-e1793.
146. Preziosa P, Pagani E, Moiola L, Rodegher M, Filippi M, Rocca MA. Occurrence and microstructural features of slowly expanding lesions on fingolimod or natalizumab treatment in multiple sclerosis. *Mult Scler*. 2021;27:1520-1532.
147. Arnold DL, Elliot C, Montalban X, Martin E, Hyvert Y, Tomic D. Effects of evobrutinib, a Bruton's tyrosine kinase inhibitor, on slowly expanding lesions: An emerging imaging marker of chronic tissue loss in multiple sclerosis. *Mult Scler*. 2021;27:3-133.
148. Elliott C, Rudko DA, Arnold DL, et al. Lesion-level correspondence and longitudinal properties of paramagnetic rim and slowly expanding lesions in multiple sclerosis. *Mult Scler*. 2023;29:680-690.
149. Owen DRJ, Matthews PM. Imaging brain microglial activation using positron emission tomography and translocator protein-specific radioligands. *Int Rev Neurobiol*. 2011;101:19-39.
150. Banati RB, Newcombe J, Gunn RN, et al. The peripheral benzodiazepine binding site in the brain in multiple sclerosis. *Brain*. 2000;123:2321-2337.
151. Rissanen E, Tuisku J, Rokka J, et al. In vivo detection of diffuse inflammation in secondary progressive multiple sclerosis using PET imaging and the radioligand 11CPK11195. *J Nucl Med*. 2014;55:939-944.
152. Giannetti P, Politis M, Su P, et al. Microglia activation in multiple sclerosis black holes predicts outcome in progressive patients: An in vivo [(11)C](R)-PK11195-PET pilot study. *Neurobiol Dis*. 2014;65:203-210.
153. Kaunzner UW, Kang Y, Monohan E, et al. Reduction of PK11195 uptake observed in multiple sclerosis lesions after natalizumab initiation. *Mult Scler Relat Disord*. 2017;15:27-33.
154. Rissanen E, Tuisku J, Vahlberg T, et al. Microglial activation, white matter tract damage, and disability in MS. *Neurol Neuroimmunol Neuroinflamm*. 2018;5:e443.
155. Sucksdorff M, Matilainen M, Tuisku J, et al. Brain TSPO-PET predicts later disease progression independent of relapses in multiple sclerosis. *Brain*. 2020;143:3318-3330.
156. Vivash L, OBrien TJ. Imaging microglial activation with TSPO PET: Lighting up neurologic diseases? *J Nucl Med*. 2016;57:165-168.
157. Erlandsson K, Dickson J, Arridge S, Atkinson D, Ourselin S, Hutton BF. MR imaging– guided partial volume correction of PET data in PET/MR imaging. *PET Clin*. 2016;11:161-177.
158. Sucksdorff M, Rissanen E, Tuisku J, et al. Evaluation of the effect of fingolimod treatment on microglial activation using serial PET imaging in multiple sclerosis. *J Nucl Med*. 2017;58:1646-1651.
159. Ratchford JN, Endres CJ, Hammoud DA, et al. Decreased microglial activation in MS patients treated with glatiramer acetate. *J Neurol*. 2012;259:1199-1205.
160. Sucksdorff M, Tuisku J, Matilainen M, et al. Natalizumab treatment reduces microglial activation in the white matter of the MS brain. *Neurol Neuroimmunol Neuroinflamm*. 2019;6:e574.
161. Kang Y, Schlyer D, Kaunzner UW, Kuceyeski A, Kothari PJ, Gauthier SA. Comparison of two different methods of image analysis for the assessment of microglial activation in patients with multiple sclerosis using (R)-[N-methyl-carbon-11] PK11195. *PLoS One*. 2018;13:e0201289.
162. Nylund M, Sucksdorff M, Matilainen M, Polvinen E, Tuisku J, Airas L. Phenotyping of multiple sclerosis lesions according to innate immune cell activation using 18 kDa translocator protein-PET. *Brain Commun*. 2022;4:fcab301.
163. Bodini B, Poirion E, Tonietto M, et al. Individual mapping of innate immune cell activation is a candidate marker of patient-specific trajectories of worsening disability in multiple sclerosis. *J Nucl Med*. 2020;61:1043-1049.
164. Hamzaoui M, Garcia J, Boffa G, et al. Positron emission tomography with [18 F]-DPA714 unveils a smoldering component in most multiple sclerosis lesions which drives disease progression. *Ann Neurol*. 2023;94:366-383.

165. Cosenza-Nashat M, Zhao ML, Suh HS, et al. Expression of the translocator protein of 18 kDa by microglia, macrophages and astrocytes based on immunohistochemical localization in abnormal human brain. *Neuropathol Appl Neurobiol*. 2009;35:306-328.
166. Nutma E, Stephenson JA, Gorter RP, et al. A quantitative neuropathological assessment of translocator protein expression in multiple sclerosis. *Brain*. 2019;142:3440-3455.
167. Nutma E, Gebro E, Marzin MC, et al. Activated microglia do not increase 18 kDa translocator protein (TSPO) expression in the multiple sclerosis brain. *Glia*. 2021;69:2447-2458.
168. Polvinen E, Matilainen M, Nylund M, Sucksdorff M, Airas LM. TSPO-Detectable chronic active lesions predict disease progression in multiple sclerosis. *Neurol Neuroimmunol Neuroinflamm*. 2023;10:e200133.
169. Chauveau F, Boutin H, Van Camp N, Dollé F, Tavitian B. Nuclear imaging of neuroinflammation: A comprehensive review of [11C]PK11195 challengers. *Eur J Nucl Med Mol Imaging*. 2008;35:2304-2319.
170. Hagens MHJ, Golla SV, Wijburg MT, et al. In vivo assessment of neuroinflammation in progressive multiple sclerosis: A proof of concept study with [18F]DPA714 PET. *J Neuroinflammation*. 2018;15:314.
171. Endres CJ, Pomper MG, James M, et al. Initial evaluation of 11C-DPA-713, a novel TSPO PET ligand, in humans. *J Nucl Med*. 2009;50:1276-1282.
172. Park E, Gallezot JD, Delgadillo A, et al. (11)C-PBR28 imaging in multiple sclerosis patients and healthy controls: Test-retest reproducibility and focal visualization of active white matter areas. *Eur J Nucl Med Mol Imaging*. 2015;42:1081-1092.
173. Singhal T, O'Connor K, Dubey S, et al. 18F-PBR06 versus 11C-PBR28 PET for assessing white matter translocator protein binding in multiple sclerosis. *Clin Nucl Med*. 2018;43:e289-e295.
174. Unterrainer M, Mahler C, Vomacka L, et al. TSPO PET with [18F]GE-180 sensitively detects focal neuroinflammation in patients with relapsing-remitting multiple sclerosis. *Eur J Nucl Med Mol Imaging*. 2018;45:1423-1431.
175. Turkheimer FE, Rizzo G, Bloomfield PS, et al. The methodology of TSPO imaging with positron emission tomography. *Biochem Soc Trans*. 2015;43:586-592.
176. Wimberley C, Lavisse S, Hillmer A, Hinz R, Turkheimer F, Zanotti-Fregonara P. Kinetic modeling and parameter estimation of TSPO PET imaging in the human brain. *Eur J Nucl Med Mol Imaging*. 2021;49:246-256.
177. Tuisku J, Plavén-Sigray P, Gaiser EC, et al. Effects of age, BMI and sex on the glial cell marker TSPO — A multicentre [11C]PBR28 HRRT PET study. *Eur J Nucl Med Mol Imaging*. 2019;46:2329-2338.
178. Reich DS, Arnold DL, Vermersch P, et al. Safety and efficacy of tolebrutinib, an oral brainpenetrant BTK inhibitor, in relapsing multiple sclerosis: A phase 2b, randomised, doubleblind, placebo-controlled trial. *Lancet Neurol*. 2021;20:729-738.
179. Zinger N, Ponath G, Sweeney E, et al. Dimethyl fumarate reduces inflammation in chronic active multiple sclerosis lesions. *Neurol Neuroimmunol Neuroinflamm*. 2022;9:e1138.
180. Efficacy and Safety of BIIB033 (Opicinumab) as an Add-on Therapy to Disease-Modifying Therapies (DMTs) in Relapsing Multiple Sclerosis (MS) (AFFINITY). ClinicalTrials.gov identifier: NCT03222973. Accessed 6 November 2023. https://clinicaltrials.gov/ct2/show/NCT03222973
181. A Study to Evaluate Ocrelizumab Treatment in Particpants With Progressive Multiple Sclerosis (CONSONANCE). ClinicalTrials.gov identifier: NCT03523858. Accessed 6 November 2023. https://clinicaltrials.gov/ct2/show/NCT03523858
182. Effect of Ocrelizumab on Neuroinflammation in Multiple Sclerosis as measured by 11CPBR28 MR-PET Imaging of Microglia Activation. ClinicalTrials.gov identifier: NCT04230174. Accessed 6 November 2023. https://clinicaltrials.gov/ct2/show/NCT04230174
183. Queen Mary University of London. ChariotMS-Cladribine to Halt Deterioration in People With advanced Multiple sclerosis (CahriotMS). ClinicalTrials.gov identifier: NCT04695080. Accessed 6 November 2023. https://clinicaltrials.gov/ct2/show/NCT04695080
184. Zivadinov R. Study to Assess the Efficacy of Mayzent on Microglia in Secondary Progressive Multiple Sclerosis. ClinicalTrials.gov identifier: NCT04925557. Accessed 6 November 2023. https://clinicaltrials.gov/ct2/show/NCT04925557
185. National Institutes of Health Clinical Center. Effect of Corticosteroids on Inflammation at the Edge of Acute Multiple Sclerosis Plaques. ClinicalTrials.gov identifier: NCT02784210. Accessed 6 November 2023. https://clinicaltrials.gov/ct2/show/NCT02784210
186. National Institutes of Health Clinical Center. Anakinra for the Treatment of Chronically Inflamed White Matter Lesions in Multiple Sclerosis. ClinicalTrials.gov identifier: NCT04025554. Accessed 6 November 2023. https://clinicaltrials.gov/ct2/show/NCT04025554
187. National Institutes of Health Clinical Center. Tolebrutinib, a Brain-penetrant Bruton s Tyrosine Kinase Inhibitor, for the Modulation of Chronically Inflamed White Matter Lesions in Multiple Sclerosis. ClinicalTrials.gov identifier: NCT04742400. Accessed 6 November 2023. https://clinicaltrials.gov/ct2/show/NCT04742400
188. Turku University Hospital. Effect of Cladribine Treatment on Microglial Activation in the CNS (CLADPET). ClinicalTrials.gov identifier: NCT04239820. Accessed 6 November 2023. https://clinicaltrials.gov/ct2/show/NCT04239820